

Spin correlations in polarizations of P-wave charmonia χ_{cJ} and impact on J/ψ polarization

Hua-Sheng Shao^(a), Kuang-Ta Chao^(a,b,c)

(a) Department of Physics and State Key Laboratory of Nuclear Physics and Technology, Peking University, Beijing 100871, China

(b) Collaborative Innovation Center of Quantum Matter, Beijing 100871, China

(c) Center for High Energy Physics, Peking University, Beijing 100871, China

Based on a general form of the effective vertex functions for the decays of P-wave charmonia χ_{cJ} , angular distribution formulas for the subsequent decays $\chi_{cJ} \rightarrow J/\psi \gamma$ decay and $J/\psi \rightarrow \mu^+ \mu^-$ are derived. The formulas are the same as those obtained in a different approach in the literature. Our formulas are expressed in a more general form, including parity violation effects and the full angular dependence of J/ψ and muon in the cascade decay $\chi_{cJ} \rightarrow J/\psi \gamma \rightarrow \mu^+ \mu^- \gamma$. The χ_{cJ} polarization observables are expressed in terms of rational functions of the spin density matrix elements of χ_{cJ} production. Generalized rotation-invariant relations for arbitrary integer-spin particles are also derived and their expressions in terms of observable angular distribution parameters are given in the χ_{c1} and χ_{c2} . To complement our previous direct- J/ψ polarization result, we also discuss the impact on the observable prompt- J/ψ polarization. As an illustrative application of our angular distribution formulas, we present the angular distributions in terms of the tree-level spin density matrix elements of χ_{c1} and χ_{c2} production in several different frames at the Large Hadron Collider. Moreover, a reweighting method is also proposed to determine the entire set of the production spin density matrix elements of the χ_{c2} , some of which disappear or are suppressed for vanishing higher-order multipole effects making the complete extraction difficult experimentally.

PACS numbers: 13.60.Le, 13.88.+e, 14.40.Pq

I. INTRODUCTION

The polarization of heavy quarkonium in hadroproduction e.g. at the Tevatron and the LHC, is a long-standing issue in heavy quarkonium physics [1]. Non-relativistic QCD (NRQCD) [2], a rigorous effective field theory founded on the nonrelativistic nature of heavy quarkonium, foresees that a $Q\bar{Q}$ pair may be formed in a color-octet (CO) state during the hard reaction at short-distances before it hadronizes into a color-singlet (CS) physical quarkonium by radiating soft gluons. In particular, the J/ψ ($c\bar{c}$ bound state with quantum number $J^{PC} = 1^{--}$), when produced at high transverse momentum (p_T), should predominantly originate from gluon fragmentation into $c\bar{c}[^3S_1^{[8]}]$, then evolve into the observed $c\bar{c}[^3S_1^{[1]}]$ [3]. The gluon fragmentation mechanism guarantees that the J/ψ is produced transversely polarized in the helicity (HX) frame when its p_T is sufficiently large. However, the data measured by the CDF [4, 5] Collaboration at the Tevatron indicate that the J/ψ is mainly unpolarized and even slightly longitudinally polarized at large p_T , up to 20 GeV. This is the “polarization puzzle” of heavy quarkonium production.

The understanding of charmonium polarization is also important for the simulations in the experimental analyses: the detector acceptance for lepton pairs from the decay of J/ψ (or other heavy quarkonia) strongly depends on the J/ψ polarization [6]. The lack of a consistent description of the polarization in the simulation of quarkonium production results in one of the largest

systematic uncertainties affecting the precision of cross section measurements.

Experimentally, measurements of direct- J/ψ production at hadron colliders are incomplete. The measured prompt J/ψ data include both direct production and feed-down contributions from χ_c and ψ' , through the decays $\chi_c \rightarrow J/\psi \gamma$ and $\psi' \rightarrow J/\psi \pi \pi$ (plus a small contribution of $\psi' \rightarrow \chi_c \gamma \rightarrow J/\psi \gamma \gamma$). Therefore, in order to compare the theoretical results with experimental data, the χ_c and ψ' yield and polarizations must also be calculated. Moreover, the χ_c meson has its own phenomenological interest. The ratio of the differential cross sections for the χ_{c1} and χ_{c2} inclusive productions at the Tevatron has been measured by the CDF Collaboration [7]. Their results show that the ratio disagrees with the spin symmetry expectation from the leading-order (LO) computation. After including the next-to-leading (NLO) QCD radiative correction [8], the asymptotic behavior of $\frac{d\sigma}{dp_T^2}$

changes from p_T^{-6} at LO to p_T^{-4} at NLO for the $^3P_J^{[1]}$ channel and, hence, becomes comparable to the contribution of $^3S_1^{[8]}$ at large p_T . The result provides an opportunity to solve the contradiction between the experiment and the theoretical prediction. The recent LHCb result [9] for $\frac{d\sigma_{\chi_{c2}}}{d\sigma_{\chi_{c1}}}$ stays within the error bars of the NLO NRQCD prediction. Surely, as in the J/ψ case, the investigation of polarization of χ_c will also be very helpful in understanding the charmonium production mechanisms in QCD.

We now briefly review the recent progress in the theory of heavy quarkonium hadroproduction. In Ref. [10], it was found that the NLO prediction for the direct- J/ψ

yield in the $^3S_1^{[1]}$ channel is 2 orders of magnitude larger than the LO one at large p_T , while NLO corrections for the CO S wave are small [11]. For the P wave, the NLO corrections for the $^3P_J^{[1]}$ channel [8] and $^3P_J^{[8]}$ channel [12–14] are found to be very large but negative. As for the polarization, the NLO QCD correction [15] for the direct- J/ψ in the CS changes it from being transverse (LO) to longitudinal (NLO) in the HX frame. This can be understood in collinear factorization up to the NLO power in $\frac{m_c^2}{p_T^2}$ [16]. However, even after including NNLO* corrections [17], in which only tree-level diagrams at α_S^5 are considered and infrared cutoffs are imposed to avoid soft and collinear divergences, theoretical predictions of CS contributions to the yields and polarizations are still in disagreement with the CDF data [4, 5]. Recently, two groups [18, 19] have presented their NLO results for the direct- J/ψ production at hadron colliders, but drawn very different conclusions due to different treatments for the fit procedure of the available data and extracted different CO long-distance matrix elements (LDMEs). The former group [18] uses a global fit, while the latter [19] just concentrates on hadroproduction, including not only the J/ψ yields but also the polarization data. In the latter approach, the predictions of yields at the LHC are in good agreement with data [20, 21] up to 70 GeV, and the J/ψ produced at the Tevatron and the LHC is found to be almost unpolarized [19].

The angular distributions of the χ_c decay into $J/\psi + \gamma$ have been studied in Ref. [22] and the authors have also calculated the spin density matrix elements (SDMEs) of χ_{c1} and χ_{c2} at the Tevatron Run I. The formulas of the angular distributions have also been derived in Ref. [23], additionally considering the subsequent decay of the J/ψ into a lepton pair. In the present paper we rederive the same expressions using a different formalism. Our formulas, like Eqs.(13) and (C1) below, can be easily extended to derive the correlations between the $\chi_c \rightarrow J/\psi\gamma$ and $J/\psi \rightarrow \mu^+\mu^-$ angular distributions. For an illustrative example to our derived results in the paper, we also compute the tree-level yields and polarizations of the χ_{c1} and χ_{c2} inclusive productions at the LHC for a center-of-mass energy of 8 TeV. Our complete NLO NRQCD predictions of χ_{c1} and χ_{c2} including yields and polarizations are given in Ref. [24].

The organization of the paper is as follows. In Sec. II, we introduce the basic kinematics and conventions used in the paper. In the next three sections, we derive the angular distributions of the J/ψ and the μ^+ from the decays of χ_{c1} and χ_{c2} . In Sec. VI, we generalize the rotation-invariant relations from the vector boson to arbitrary integer-spin particles. In Sec. VII, we estimate the impact of the feed-down contributions from χ_c and ψ' on the prompt- J/ψ polarization. In Sec. VIII, we present an example to illustrate our derived formulas. Finally, the conclusion is drawn in the last section. General expressions of the decay angular distributions for spin-1 and spin-2 bosons taking into account higher-order radi-

ation multipoles and allowing for parity-violating effects, are presented in the Appendixes A, B, C. A reweighting method is also proposed to extract the complete set of the SDMEs of the χ_{c2} in Appendix D.

II. KINEMATICS AND CONVENTIONS

In this section, we introduce the conventions and kinematics for our derivations performed in the following sections. Apart from $\chi_c \rightarrow J/\psi + \gamma$, we also consider the subsequent $J/\psi \rightarrow \mu^+\mu^-$. The spin quantization axis \vec{s} can be chosen arbitrarily in the rest frame of the decaying particle. Generally, the polarization vectors for a massive spin-1 particle are

$$\begin{aligned}\epsilon_0^\mu &= (|\vec{k}|, E \sin \theta \cos \phi, E \sin \theta \sin \phi, E \cos \theta)/m, \\ \epsilon_\pm^\mu &= \frac{e^{\mp i\gamma}}{\sqrt{2}} (0, \mp \cos \theta \cos \phi + i \sin \phi, \\ &\quad \mp \cos \theta \sin \phi - i \cos \phi, \pm \sin \theta),\end{aligned}\quad (1)$$

where θ and ϕ are the polar and azimuthal decay angles with respect to \vec{s} and a chosen plane,¹ and the symbol γ can be chosen as an arbitrary real number. E , \vec{k} , and m are the particle's energy, momentum, and mass. We set $\gamma = -\phi$ here. For a spin-2 tensor particle, its spin wave functions can be constructed from the spin-1 polarization four-vectors as

$$\epsilon_\lambda^{\mu\nu} = \sum_{\lambda_1, \lambda_2=-1}^1 \langle 1, \lambda_1; 1, \lambda_2 | 2, \lambda \rangle \epsilon_{\lambda_1}^\mu \epsilon_{\lambda_2}^\nu, \quad (2)$$

where $\langle 1, \lambda_1; 1, \lambda_2 | 2, \lambda \rangle$ are the Clebsch-Gordan coefficients, and $\lambda, \lambda_1, \lambda_2$ denote the angular distribution components along the spin-quantization axis \vec{s} . Thus, we have the identities $p_\mu \epsilon_\lambda^\mu = p_\mu \epsilon_\lambda^{\mu\nu} = p_\nu \epsilon_\lambda^{\mu\nu} = (\epsilon_\lambda)^\mu_\mu = 0$ and $\epsilon_\lambda^{\mu\nu} = \epsilon_\lambda^{\nu\mu}$.

The $\chi_{cJ} \rightarrow J/\psi\gamma$ angular distribution can be written in terms of the χ_{cJ} production SDMEs $\rho_{\lambda\lambda'}$ and of the decay SDMEs $D_{\lambda\lambda'}$,

$$\mathcal{W}(\theta, \phi) = \sum_{\lambda, \lambda'=-J}^J \rho_{\lambda\lambda'} D_{\lambda\lambda'}(\theta, \phi), \quad (3)$$

where θ and ϕ are the angles parameterizing the J/ψ direction in the χ_{cJ} rest frame. Here, $\rho_{\lambda\lambda'}$ and $D_{\lambda\lambda'}$ represent the production and decay amplitudes of the χ_{cJ} with angular momentum projector component λ along \vec{s} multiplied by the corresponding complex conjugate amplitudes with component λ' .

¹ The plane is an important component to define the polarization frames. At the end of this section, we will fix our chosen polarization axis and corresponding plane.

Several polarization frame definitions have been used in the literature to fully describe the polarization of heavy quarkonium [25], i.e. the HX (recoil or s-channel helicity) frame, the Collins-Soper frame, the Gottfried-Jackson frame, and the target frame.² In the HX frame, \vec{s} is chosen as the flight direction of the decaying quarkonium. In the Collins-Soper frame,

$$\vec{s} = (\vec{p}_1/|\vec{p}_1| - \vec{p}_2/|\vec{p}_2|)/|\vec{p}_1/|\vec{p}_1| - \vec{p}_2/|\vec{p}_2||, \quad (4)$$

where \vec{p}_1 and \vec{p}_2 denote the momenta of the two initial state colliding particles in the rest frame of the decaying quarkonium. In the Gottfried-Jackson frame, $\vec{s} = \frac{\vec{p}_1}{|\vec{p}_1|}$, and in the target frame, $\vec{s} = -\frac{\vec{p}_2}{|\vec{p}_2|}$. All the definitions of the X, Y, Z coordinates can be found in Ref. [25]. In particular, the Y coordinate points in the direction of $\vec{p}_1 \times (-\vec{p}_2)$ in the χ_c rest frame.

III. ANGULAR DISTRIBUTION OF $\chi_{c1} \rightarrow J/\psi\gamma$

The general vertex function for the decay of a vector or axial vector particle into two vector particles can be expressed as

$$\begin{aligned} \mathcal{M}(V_0 \rightarrow V_1 V_2) = & f_1 (\epsilon_{V_0} \cdot \epsilon_{V_1}^*) [\epsilon_{V_2}^* \cdot (-p_{V_0} - p_{V_1})] \\ & + f_2 (\epsilon_{V_0} \cdot \epsilon_{V_2}^*) [\epsilon_{V_1}^* \cdot (p_{V_0} + p_{V_2})] \\ & + f_3 (\epsilon_{V_1}^* \cdot \epsilon_{V_2}^*) [\epsilon_{V_0} \cdot (p_{V_1} - p_{V_2})] \\ & + f_4 [\epsilon_{V_0} \cdot (p_{V_1} - p_{V_2})] \\ & \quad [\epsilon_{V_1}^* \cdot (p_{V_0} + p_{V_2})] [\epsilon_{V_2}^* \cdot (p_{V_0} + p_{V_1})] \\ & + f_5 i \epsilon_{\epsilon_{V_0} \epsilon_{V_1}^* \epsilon_{V_2}^* p_{V_0}} \\ & + f_6 [\epsilon_{V_1}^* \cdot (p_{V_0} + p_{V_2})] i \epsilon_{\epsilon_{V_0} \epsilon_{V_2}^* p_{V_0} p_{V_2}} \\ & + f_7 [\epsilon_{V_2}^* \cdot (p_{V_0} + p_{V_1})] i \epsilon_{\epsilon_{V_0} \epsilon_{V_1}^* p_{V_0} p_{V_1}}, \end{aligned} \quad (5)$$

where

$$p_{V_0} = p_{V_1} + p_{V_2}.$$

and $\epsilon_{\mu\nu\rho\sigma}$ is the antisymmetric Levi-Civita tensor. A special notation about the vector contracting with the Levi-Civita tensor is used, for example, $\epsilon_{\mu\nu\rho k} \equiv \epsilon_{\mu\nu\rho\sigma} k^\sigma$. Specifically, in the case of $\chi_{c1}(1^{++}) \rightarrow J/\psi(1^{--})\gamma(1^{--})$, the f_1, f_2, f_3, f_4 terms and the f_7 term can be dropped because of parity conservation in QED and the absence of a longitudinal polarization component for the photon. If we just consider the electric dipole (E1) transition, which is the dominant contribution according to the velocity scaling rule in NRQCD, the f_6 term can also be neglected. Therefore, we calculate the helicity amplitudes $\mathcal{M}_{\lambda_{\chi_{c1}} \lambda_{J/\psi} \lambda_\gamma}$

for $\chi_{c1} \rightarrow J/\psi\gamma$ as

$$\begin{aligned} \mathcal{M}_{+++} &= \mathcal{M}_{---}^* = \frac{m_{\chi_{c1}} e^{-i\phi} \sin \theta}{\sqrt{2}}, \\ \mathcal{M}_{+--} &= \mathcal{M}_{-++}^* = -\frac{m_{\chi_{c1}} e^{3i\phi} \sin \theta}{\sqrt{2}}, \\ \mathcal{M}_{+0+} &= -\mathcal{M}_{-0-} = -\frac{(m_{\chi_{c1}}^2 + m_{J/\psi}^2) \sin^2 \frac{\theta}{2}}{2m_{J/\psi}}, \\ \mathcal{M}_{+0-} &= -\mathcal{M}_{-0+}^* = \frac{(m_{\chi_{c1}}^2 + m_{J/\psi}^2) e^{2i\phi} \cos^2 \frac{\theta}{2}}{2m_{J/\psi}}, \\ \mathcal{M}_{0++} &= -\mathcal{M}_{0--}^* = -m_{\chi_{c1}} e^{-2i\phi} \cos \theta, \\ \mathcal{M}_{00+} &= \mathcal{M}_{00-}^* = \frac{(m_{\chi_{c1}}^2 + m_{J/\psi}^2) e^{-i\phi} \sin \theta}{2\sqrt{2}m_{J/\psi}}, \end{aligned} \quad (6)$$

where a factor $f_5(m_{\chi_{c1}}^2 - m_{J/\psi}^2)$ common to all amplitudes has been omitted. The decay SDMEs are obtained as $D_{\lambda\lambda'} = \sum_{\lambda_{J/\psi}, \lambda_\gamma} \mathcal{M}_{\lambda\lambda_{J/\psi}\lambda_\gamma} \mathcal{M}_{\lambda'\lambda_{J/\psi}\lambda_\gamma}^*$. Using these ingredients [i.e. Eqs.(3) and (6)] and assuming $m_{\chi_{c1}} = m_{J/\psi}$, we can work out the general form of the angular distribution of $\chi_{c1} \rightarrow J/\psi\gamma$:

$$\begin{aligned} \mathcal{W}^{\chi_{c1} \rightarrow J/\psi\gamma}(\theta, \phi) \propto & \frac{N_{\chi_{c1} \rightarrow J/\psi\gamma}}{3 + \lambda_\theta} (1 + \lambda_\theta \cos^2 \theta \\ & + \lambda_\phi \sin^2 \theta \cos 2\phi + \lambda_{\theta\phi} \sin 2\theta \cos \phi \\ & + \lambda_\phi^\perp \sin^2 \theta \sin 2\phi + \lambda_{\theta\phi}^\perp \sin 2\theta \sin \phi), \end{aligned} \quad (7)$$

with

$$\begin{aligned} \lambda_\theta &= \frac{3\rho_{0,0} - N_{\chi_{c1}}}{3N_{\chi_{c1}} - \rho_{0,0}}, \lambda_\phi = -\frac{2\Re\rho_{1,-1}}{3N_{\chi_{c1}} - \rho_{0,0}}, \\ \lambda_{\theta\phi} &= -\frac{\sqrt{2}(\Re\rho_{1,0} - \Re\rho_{-1,0})}{3N_{\chi_{c1}} - \rho_{0,0}}, \\ \lambda_\phi^\perp &= \frac{2\Im\rho_{1,-1}}{3N_{\chi_{c1}} - \rho_{0,0}}, \lambda_{\theta\phi}^\perp = \frac{\sqrt{2}(\Im\rho_{1,0} + \Im\rho_{-1,0})}{3N_{\chi_{c1}} - \rho_{0,0}}, \end{aligned} \quad (8)$$

where $\rho_{i,j}$ are SDMEs for the χ_{c1} yields and $N_{\chi_{c1}} = \rho_{1,1} + \rho_{0,0} + \rho_{-1,-1}$.

IV. ANGULAR DISTRIBUTION OF $\chi_{c2} \rightarrow J/\psi\gamma$

Similarly, in the χ_{c2} case, we can write down the general vertex function for a spin-2 tensor particle T decaying into two vector particles

$$\begin{aligned} \mathcal{M}(T \rightarrow V_1 V_2) = & g_1 \epsilon_{V_2}^* \cdot \epsilon_T \cdot \epsilon_{V_1}^* \\ & + g_2 [(p_{V_1} - p_{V_2}) \cdot \epsilon_T \cdot \epsilon_{V_1}^*] [\epsilon_{V_2}^* \cdot (-p_T - p_{V_1})] \\ & + g_3 [(p_{V_1} - p_{V_2}) \cdot \epsilon_T \cdot \epsilon_{V_2}^*] [\epsilon_{V_1}^* \cdot (p_T + p_{V_2})] \\ & + g_4 [(p_{V_1} - p_{V_2}) \cdot \epsilon_T \cdot (p_{V_1} - p_{V_2})] (\epsilon_{V_1}^* \cdot \epsilon_{V_2}^*) \\ & + g_5 [(p_{V_1} - p_{V_2}) \cdot \epsilon_T \cdot (p_{V_1} - p_{V_2})] \\ & \quad [\epsilon_{V_1}^* \cdot (p_T + p_{V_2})] [\epsilon_{V_2}^* \cdot (p_T + p_{V_1})] \\ & + \text{Levi-Civita terms}, \end{aligned} \quad (9)$$

² Another useful frame is the “perpendicular helicity frame” [26, 27]. It has been used in the Υ polarization measurement [28] by the CMS Collaboration.

where $p_T = p_{V_1} + p_{V_2}$. Because of parity conservation, we drop the Levi-Civita terms in $\chi_{c2}(2^{++}) \rightarrow J/\psi(1^{--})\gamma(1^{--})$. The g_2, g_3, g_4, g_5 terms can also be ignored in consideration of the fact that we only include the leading-order contribution, i.e., the E1 transition, and these terms are suppressed by $(m_{\chi_{c2}}^2 - m_{J/\psi}^2)^2$ as compared to the g_1 term. Moreover, some of these terms vanish exactly when the photon is transversely polarized. Thus, the helicity amplitudes $\mathcal{M}_{\lambda_{\chi_{c2}} \lambda_{J/\psi} \lambda_\gamma}$ for $\chi_{c2} \rightarrow J/\psi \gamma$ become

$$\begin{aligned}
\mathcal{M}_{2++} &= \mathcal{M}_{-2--} = \frac{\sin^2 \theta}{4}, \\
\mathcal{M}_{2+-} &= \mathcal{M}_{-2-+}^* = e^{2i\phi} \cos^4 \frac{\theta}{2}, \\
\mathcal{M}_{2--} &= \mathcal{M}_{-2++}^* = \frac{e^{4i\phi} \sin^2 \theta}{4}, \\
\mathcal{M}_{2-+} &= \mathcal{M}_{-2+-}^* = e^{2i\phi} \sin^4 \frac{\theta}{2}, \\
\mathcal{M}_{20+} &= -\mathcal{M}_{-20-}^* = -\frac{m_{\chi_{c2}}^2 + m_{J/\psi}^2}{\sqrt{2}m_{\chi_{c2}}m_{J/\psi}} e^{i\phi} \sin^3 \frac{\theta}{2} \cos \frac{\theta}{2}, \\
\mathcal{M}_{20-} &= -\mathcal{M}_{-20+}^* = -\frac{m_{\chi_{c2}}^2 + m_{J/\psi}^2}{\sqrt{2}m_{\chi_{c2}}m_{J/\psi}} e^{3i\phi} \cos^3 \frac{\theta}{2} \sin \frac{\theta}{2}, \\
\mathcal{M}_{1++} &= -\mathcal{M}_{-1--}^* = -\frac{e^{-i\phi} \sin 2\theta}{4}, \\
\mathcal{M}_{1+-} &= -\mathcal{M}_{-1-+}^* = 2e^{i\phi} \cos^3 \frac{\theta}{2} \sin \frac{\theta}{2}, \\
\mathcal{M}_{1--} &= -\mathcal{M}_{-1++}^* = -\frac{e^{3i\phi} \sin 2\theta}{4}, \\
\mathcal{M}_{1-+} &= -\mathcal{M}_{-1+-}^* = -2e^{i\phi} \sin^3 \frac{\theta}{2} \cos \frac{\theta}{2}, \\
\mathcal{M}_{10+} &= \mathcal{M}_{-10-} = \frac{m_{\chi_{c2}}^2 + m_{J/\psi}^2}{2\sqrt{2}m_{\chi_{c2}}m_{J/\psi}} \sin^2 \frac{\theta}{2} (1 + 2 \cos \theta), \\
\mathcal{M}_{10-} &= \mathcal{M}_{-10+}^* = \frac{m_{\chi_{c2}}^2 + m_{J/\psi}^2}{2\sqrt{2}m_{\chi_{c2}}m_{J/\psi}} e^{2i\phi} \cos^2 \frac{\theta}{2} (2 \cos \theta - 1), \\
\mathcal{M}_{0++} &= \mathcal{M}_{0--}^* = \frac{e^{-2i\phi} (1 + 3 \cos 2\theta)}{4\sqrt{6}}, \\
\mathcal{M}_{0+-} &= \mathcal{M}_{0-+} = \frac{3 \sin^2 \theta}{2\sqrt{6}}, \\
\mathcal{M}_{00+} &= -\mathcal{M}_{00-}^* = -\frac{\sqrt{3}(m_{\chi_{c2}}^2 + m_{J/\psi}^2)}{8m_{\chi_{c2}}m_{J/\psi}} e^{-i\phi} \sin 2\theta. \quad (10)
\end{aligned}$$

The angular distribution of the $\chi_{c2} \rightarrow J/\psi \gamma$ decay has, in the E1 approximation and assuming $m_{\chi_{c2}} = m_{J/\psi}$, the same general expression of the $\chi_{c1} \rightarrow J/\psi \gamma$ case:

$$\begin{aligned}
\mathcal{W}^{\chi_{c2} \rightarrow J/\psi \gamma}(\theta, \phi) &\propto \frac{N_{\chi_{c2} \rightarrow J/\psi \gamma}}{3 + \lambda_\theta} (1 + \lambda_\theta \cos^2 \theta) \\
&+ \lambda_\phi \sin^2 \theta \cos 2\phi + \lambda_{\theta\phi} \sin 2\theta \cos \phi \\
&+ \lambda_\phi^\perp \sin^2 \theta \sin 2\phi + \lambda_{\theta\phi}^\perp \sin 2\theta \sin \phi
\end{aligned} \quad (11)$$

with

$$\begin{aligned}
\lambda_\theta &= \frac{6N_{\chi_{c2}} - 9(\rho_{1,1} + \rho_{-1,-1}) - 12\rho_{0,0}}{6N_{\chi_{c2}} + 3(\rho_{1,1} + \rho_{-1,-1}) + 4\rho_{0,0}}, \\
\lambda_\phi &= \frac{2\sqrt{6}(\Re\rho_{2,0} + \Re\rho_{-2,0}) + 6\Re\rho_{1,-1}}{6N_{\chi_{c2}} + 3(\rho_{1,1} + \rho_{-1,-1}) + 4\rho_{0,0}}, \\
\lambda_{\theta\phi} &= \frac{6(\Re\rho_{2,1} - \Re\rho_{-2,-1}) + \sqrt{6}(\Re\rho_{1,0} - \Re\rho_{-1,0})}{6N_{\chi_{c2}} + 3(\rho_{1,1} + \rho_{-1,-1}) + 4\rho_{0,0}}, \\
\lambda_\phi^\perp &= -\frac{2\sqrt{6}(\Im\rho_{2,0} - \Im\rho_{-2,0}) + 6\Im\rho_{1,-1}}{6N_{\chi_{c2}} + 3(\rho_{1,1} + \rho_{-1,-1}) + 4\rho_{0,0}}, \\
\lambda_{\theta\phi}^\perp &= -\frac{6(\Im\rho_{2,1} + \Im\rho_{-2,-1}) + \sqrt{6}(\Im\rho_{1,0} + \Im\rho_{-1,0})}{6N_{\chi_{c2}} + 3(\rho_{1,1} + \rho_{-1,-1}) + 4\rho_{0,0}}, \\
N_{\chi_{c2}} &= \rho_{2,2} + \rho_{1,1} + \rho_{0,0} + \rho_{-1,-1} + \rho_{-2,-2}. \quad (12)
\end{aligned}$$

If the magnetic quadrupole (M2) and electric octupole (E3) contributions are also taken into account by keeping the relevant terms in the vertex functions, the expression of the angular distribution acquires further terms in the χ_{c2} case while, both for χ_{c1} and χ_{c2} , the existing terms are modified. The modifications depend on one additional coefficient (expressing the fractional M2 amplitude contribution) in the χ_{c1} case and on two additional coefficients (M2 and E3 contributions) in the χ_{c2} case. If these coefficients are not $< \mathcal{O}(1\%)$, they can modify the angular distributions significantly [23]. However, inconsistencies in their current experimental determinations exist [29–32]. The complete formulas for the angular distributions including the higher-order multipole effects are presented in the appendixes, while only the E1 transition is considered, for simplicity, throughout the body of the paper.

Our results [Eqs.(8) and (12)] are exactly the same as those given in Refs. [22, 23]. Actually, our derivations, which are based on the general effective decay vertex functions, are equivalent to those obtained there using the angular momentum conservation, since the effective amplitudes written by us are also originated from general considerations on the spins of the involved particles.

V. LEPTON DISTRIBUTION IN

$$\chi_{cJ} \rightarrow J/\psi \gamma \rightarrow \mu^+ \mu^- \gamma$$

We are now in a position to investigate the μ^+ angular distributions from the cascade decay $\chi_{cJ} \rightarrow J/\psi \gamma \rightarrow \mu^+ \mu^- \gamma$.

We start from a general formalism to study it. We denote with \vec{s}_1 and \vec{s}_2 the quantization axes of the χ_{cJ} and of the J/ψ , respectively. The general form of the angular distribution of the μ^+ is

$$\begin{aligned}
&\mathcal{W}^{\chi_{cJ} \rightarrow J/\psi \gamma \rightarrow \mu^+ \mu^- \gamma}(\theta', \phi') \\
&= \int d^2\Omega[\theta, \phi] \rho_{J_z, J_z'}^{\chi_{cJ}} \mathcal{M}_{J_z, J_z' \lambda_\gamma}^{\chi_{cJ} \rightarrow J/\psi \gamma}(\theta, \phi) \mathcal{M}_{s_z \lambda_\mu + \lambda_{\mu^-}}^{J/\psi \rightarrow \mu^+ \mu^-}(\theta', \phi') \\
&\quad \left(\mathcal{M}_{J_z' s_z' \lambda_\gamma}^{\chi_{cJ} \rightarrow J/\psi \gamma}(\theta, \phi) \mathcal{M}_{s_z' \lambda_\mu + \lambda_{\mu^-}}^{J/\psi \rightarrow \mu^+ \mu^-}(\theta', \phi') \right)^*, \quad (13)
\end{aligned}$$

where the $\rho_{J_z, J'_z}^{\chi_{cJ}}$ coefficients are the production SDMEs of the χ_{cJ} , $\mathcal{M}_{J_z s_z \lambda_\gamma}^{\chi_{cJ} \rightarrow J/\psi \gamma}$, $\mathcal{M}_{s_z \lambda_{\mu^+} \lambda_{\mu^-}}^{J/\psi \rightarrow \mu^+ \mu^-}$ are the amplitudes of the two successive decays,³ J_z is the χ_{cJ} angular momentum projection with respect to \vec{s}_1 , s_z the J/ψ angular momentum projection with respect to \vec{s}_2 , $\lambda_\gamma, \lambda_{\mu^+}, \lambda_{\mu^-}$ the photon and lepton helicities. The angles θ and ϕ define the J/ψ direction in the χ_{cJ} rest frame with respect to \vec{s}_1 . θ' and ϕ' determine the μ^+ direction in the J/ψ rest frame with respect to \vec{s}_2 . Indices appearing twice imply a summation, with $J_z, J'_z = \pm J, \pm(J-1), \dots, 0$, $s_z, s'_z = \pm 1, 0$, and $\lambda_\gamma, \lambda_{\mu^+}, \lambda_{\mu^-} = \pm 1$.

We will consider two different definitions of \vec{s}_2 . In the first option, \vec{s}_2 is the flight direction of the J/ψ in the rest frame of the χ_{cJ} . The $J/\psi \rightarrow \mu^+ \mu^-$ angular distribution can be parametrized in the same form of Eqs.(7) and (11), with five observable coefficients depending on the χ_{cJ} SDMEs $\rho_{J_z, J'_z}^{\chi_{cJ}}$:

$$\begin{aligned} \lambda_{\theta'}^{\chi_{c1}} &= -\frac{1}{3}, \lambda_{\phi'}^{\chi_{c1}} = \lambda_{\phi'}^{\perp \chi_{c1}} = 0, \\ \lambda_{\theta' \phi'}^{\chi_{c1}} &= \frac{\sqrt{2}(\Re(\rho_{1,0}^{\chi_{c1}}) - \Re(\rho_{-1,0}^{\chi_{c1}}))}{12N_{\chi_{c1}}}, \\ \lambda_{\theta' \phi'}^{\perp \chi_{c1}} &= -\frac{\sqrt{2}(\Im(\rho_{1,0}^{\chi_{c1}}) + \Im(\rho_{-1,0}^{\chi_{c1}}))}{12N_{\chi_{c1}}}, \\ \lambda_{\theta'}^{\chi_{c2}} &= \frac{1}{13}, \\ \lambda_{\phi'}^{\chi_{c2}} &= \frac{7\sqrt{6}(\Re\rho_{0,2}^{\chi_{c2}} + \Re\rho_{0,-2}^{\chi_{c2}}) + 12\Re\rho_{1,-1}^{\chi_{c2}}}{78N_{\chi_{c2}}}, \\ \lambda_{\theta' \phi'}^{\chi_{c2}} &= \frac{\sqrt{6}(\Re\rho_{-1,0}^{\chi_{c2}} - \Re\rho_{1,0}^{\chi_{c2}}) + 24(\Re\rho_{-2,-1}^{\chi_{c2}} - \Re\rho_{2,1}^{\chi_{c2}})}{156N_{\chi_{c2}}}, \\ \lambda_{\phi'}^{\perp \chi_{c2}} &= \frac{7\sqrt{6}(\Im\rho_{0,2}^{\chi_{c2}} - \Im\rho_{0,-2}^{\chi_{c2}}) - 12\Im\rho_{1,-1}^{\chi_{c2}}}{78N_{\chi_{c2}}}, \\ \lambda_{\theta' \phi'}^{\perp \chi_{c2}} &= \frac{\sqrt{6}(\Im\rho_{-1,0}^{\chi_{c2}} + \Im\rho_{1,0}^{\chi_{c2}}) + 24(\Im\rho_{-2,-1}^{\chi_{c2}} + \Im\rho_{2,1}^{\chi_{c2}})}{156N_{\chi_{c2}}}, \end{aligned} \quad (14)$$

with $N_{\chi_{cJ}} = \sum_{\lambda=-J}^J \rho_{\lambda\lambda}^{\chi_{cJ}}$. We see that the same results can be obtained in another formalism using the language of angular momentum theory. The spin correlations between the χ_{cJ} production SDMEs $\rho_{J_z, J'_z}^{\chi_{cJ}}$, referred to the quantization axis \vec{s}_1 and the SDMEs of the J/ψ coming from χ_{cJ} , $\rho_{s_z, s'_z}^{\chi_{cJ} \rightarrow J/\psi \gamma}$ referred to \vec{s}_2 , can be expressed as

$$\begin{aligned} \rho_{s_z, s'_z}^{\chi_{cJ} \rightarrow J/\psi \gamma} &= \frac{3}{8\pi} \int d\Omega[\theta, \phi] \rho_{J_z, J'_z}^{\chi_{cJ}} \mathcal{D}_{J_z, I_z}^{J*} \mathcal{D}_{J'_z, I'_z}^J \quad (15) \\ \langle 1, \lambda_\gamma; 1, s_z | J, I_z \rangle \langle J, I'_z | 1, \lambda_\gamma; 1, s'_z \rangle &\text{Br}(\chi_{cJ} \rightarrow J/\psi \gamma), \end{aligned}$$

where implicit summations run over $J_z, J'_z, I_z, I'_z = \pm J, \pm(J-1), \dots, 0$ and over $\lambda_\gamma = \pm 1$, $\text{Br}(\chi_{cJ} \rightarrow J/\psi \gamma)$ is

the branching ratio of the radiative decay and $\mathcal{D}_{J_z, J'_z}^J \equiv \mathcal{D}_{J_z, J'_z}^J(-\phi, \theta, \phi) = e^{i\phi(J_z - J'_z)} d_{J_z, J'_z}^J(\theta)$, $d_{J_z, J'_z}^J(\theta)$ being the well-known Wigner d function

$$\begin{aligned} d_{J_z, J'_z}^J(\theta) &= \sum_{k=\max(0, J'_z - J_z)}^{\min(J + J'_z, J - J_z)} (-)^{k - J'_z + J_z} \quad (16) \\ &\times \frac{\sqrt{(J + J'_z)!(J - J'_z)!(J + J_z)!(J - J_z)!}}{(J + J'_z - k)!k!(J - J_z - k)!(k - J'_z + J_z)!} \\ &\times \left(\cos \frac{\theta}{2}\right)^{2J - 2k + J'_z - J_z} \left(\sin \frac{\theta}{2}\right)^{2k - J'_z + J_z}. \end{aligned}$$

One can easily verify that after substituting $\rho_{s_z, s'_z}^{\chi_{cJ} \rightarrow J/\psi \gamma}$ calculated from the above equation into the well-known expression of the angular distribution of the muon from $J/\psi \rightarrow \mu^+ \mu^-$,

$$\begin{aligned} \lambda_{\theta'}^{J/\psi} &= \frac{N_{J/\psi} - 3\rho_{0,0}^{J/\psi}}{N_{J/\psi} + \rho_{0,0}^{J/\psi}}, \\ \lambda_{\phi'}^{J/\psi} &= \frac{2\Re\rho_{1,-1}^{J/\psi}}{N_{J/\psi} + \rho_{0,0}^{J/\psi}}, \\ \lambda_{\theta' \phi'}^{J/\psi} &= \frac{\sqrt{2}(\Re\rho_{1,0}^{J/\psi} - \Re\rho_{-1,0}^{J/\psi})}{N_{J/\psi} + \rho_{0,0}^{J/\psi}}, \\ \lambda_{\theta' \phi'}^{\perp J/\psi} &= -\frac{2\Im\rho_{1,-1}^{J/\psi}}{N_{J/\psi} + \rho_{0,0}^{J/\psi}}, \\ \lambda_{\phi'}^{\perp J/\psi} &= -\frac{\sqrt{2}(\Im\rho_{1,0}^{J/\psi} + \Im\rho_{-1,0}^{J/\psi})}{N_{J/\psi} + \rho_{0,0}^{J/\psi}}, \end{aligned} \quad (17)$$

the expressions in Eq.(14) are recovered.

As a second option, \vec{s}_2 is chosen as coinciding with \vec{s}_1 . The J/ψ spin state $|1, s_z\rangle$ with respect to \vec{s}_2 is no longer its helicity state, like in the first case. This option is actually a much “easier” choice for the experiment, at least at not very low J/ψ momentum, because it does not require the use of the photon momentum, and it actually coincides with the usual set of reference frames adopted in the study of prompt J/ψ [23]. With a direct calculation following Eq.(13), we obtain

$$\begin{aligned} \lambda_{\theta'}^{\chi_{c1}} &= \frac{-N_{\chi_{c1}} + 3\rho_{0,0}^{\chi_{c1}}}{3N_{\chi_{c1}} - \rho_{0,0}^{\chi_{c1}}}, \\ \lambda_{\phi'}^{\chi_{c1}} &= -\frac{2\Re\rho_{1,-1}^{\chi_{c1}}}{3N_{\chi_{c1}} - \rho_{0,0}^{\chi_{c1}}}, \\ \lambda_{\theta' \phi'}^{\chi_{c1}} &= -\frac{\sqrt{2}(\Re\rho_{1,0}^{\chi_{c1}} - \Re\rho_{-1,0}^{\chi_{c1}})}{3N_{\chi_{c1}} - \rho_{0,0}^{\chi_{c1}}}, \\ \lambda_{\phi'}^{\perp \chi_{c1}} &= \frac{2\Im\rho_{1,-1}^{\chi_{c1}}}{3N_{\chi_{c1}} - \rho_{0,0}^{\chi_{c1}}}, \\ \lambda_{\theta' \phi'}^{\perp \chi_{c1}} &= \frac{\sqrt{2}(\Im\rho_{1,0}^{\chi_{c1}} + \Im\rho_{-1,0}^{\chi_{c1}})}{3N_{\chi_{c1}} - \rho_{0,0}^{\chi_{c1}}}, \end{aligned} \quad (18)$$

³ We use the general vector current amplitudes for the J/ψ decay into a muon pair.

$$\begin{aligned}
\lambda_{\theta'}^{\chi_{c2}} &= \frac{6N_{\chi_{c2}} - 9(\rho_{1,1}^{\chi_{c2}} + \rho_{-1,-1}^{\chi_{c2}}) - 12\rho_{0,0}^{\chi_{c2}}}{6N_{\chi_{c2}} + 3(\rho_{1,1}^{\chi_{c2}} + \rho_{-1,-1}^{\chi_{c2}}) + 4\rho_{0,0}^{\chi_{c2}}}, \\
\lambda_{\phi'}^{\chi_{c2}} &= \frac{2\sqrt{6}(\Re\rho_{2,0}^{\chi_{c2}} + \Re\rho_{-2,0}^{\chi_{c2}}) + 6\Re\rho_{1,-1}^{\chi_{c2}}}{6N_{\chi_{c2}} + 3(\rho_{1,1}^{\chi_{c2}} + \rho_{-1,-1}^{\chi_{c2}}) + 4\rho_{0,0}^{\chi_{c2}}}, \\
\lambda_{\theta'\phi'}^{\chi_{c2}} &= \frac{6(\Re\rho_{2,1}^{\chi_{c2}} - \Re\rho_{-2,-1}^{\chi_{c2}}) + \sqrt{6}(\Re\rho_{1,0}^{\chi_{c2}} - \Re\rho_{-1,0}^{\chi_{c2}})}{6N_{\chi_{c2}} + 3(\rho_{1,1}^{\chi_{c2}} + \rho_{-1,-1}^{\chi_{c2}}) + 4\rho_{0,0}^{\chi_{c2}}}, \\
\lambda_{\phi'}^{\perp\chi_{c2}} &= \frac{2\sqrt{6}(\Im\rho_{0,2}^{\chi_{c2}} - \Im\rho_{0,-2}^{\chi_{c2}}) - 6\Im\rho_{1,-1}^{\chi_{c2}}}{6N_{\chi_{c2}} + 3(\rho_{1,1}^{\chi_{c2}} + \rho_{-1,-1}^{\chi_{c2}}) + 4\rho_{0,0}^{\chi_{c2}}}, \\
\lambda_{\theta'\phi'}^{\perp\chi_{c2}} &= \frac{6(\Im\rho_{1,2}^{\chi_{c2}} + \Im\rho_{-1,-2}^{\chi_{c2}}) + \sqrt{6}(\Im\rho_{0,1}^{\chi_{c2}} + \Im\rho_{0,-1}^{\chi_{c2}})}{6N_{\chi_{c2}} + 3(\rho_{1,1}^{\chi_{c2}} + \rho_{-1,-1}^{\chi_{c2}}) + 4\rho_{0,0}^{\chi_{c2}}}.
\end{aligned}$$

One can also derive these expressions by combining

$$\begin{aligned}
\rho_{s_z, s'_z}^{\chi_{cJ} \rightarrow J/\psi\gamma} &\propto \sum_{l_z = \pm 1, 0} \sum_{J_z, J'_z} \langle 1, l_z; 1, s_z | J, J_z \rangle \\
&\langle J, J'_z | 1, l_z; 1, s'_z \rangle \rho_{J_z, J'_z}^{\chi_{cJ}} \text{Br}(\chi_{cJ} \rightarrow J/\psi\gamma) \quad (19)
\end{aligned}$$

and Eq.(17). It is interesting to note that the expressions for the $J/\psi \rightarrow \mu^+\mu^-$ distributions obtained with this option for \vec{s}_2 are exactly identical (having the same dependence on the χ_{cJ} production SDMEs) to the expressions obtained before for the $\chi_{cJ} \rightarrow J/\psi\gamma$ distributions. This is only rigorously true when only the E1 transitions are considered. As is discussed quantitatively in Ref. [23] [whose results are reproduced by Eq.(18)], the $J/\psi \rightarrow \mu^+\mu^-$ distributions are only mildly corrected by the additional M2 and E3 contributions, while the $\chi_{cJ} \rightarrow J/\psi\gamma$ distributions are quite sensitive to them.

VI. ROTATION INVARIANT RELATIONS FOR ARBITRARY INTEGER-SPIN PARTICLES

The partonic Drell-Yan process in perturbative QCD obeys the well-know Lam-Tung identity [33], which states that the coefficients λ_θ and λ_ϕ of the lepton angular distribution from the Drell-Yan process satisfy $\lambda_\theta + 4\lambda_\phi = 1$. Its theoretical relevance is that the relation remains unchanged up to $\mathcal{O}(\alpha_s^2)$ corrections [34] and receives relatively small corrections even by resummation [35]. The distinctive feature of the identity is that it is independent of the chosen orientation of the spin axis. It was later pointed out by the authors of Ref. [36] that the rotation invariance of the Lam-Tung relation is a general consequence of the rotational covariance of $J = 1$ angular momentum eigenstates. They presented an expression formally analogous to the Lam-Tung identity for a $J = 1$ boson decaying into a fermion pair with the only assumption that the spin-quantization axis \vec{s} should be set in the production plane, i.e., $F_1 = \frac{1+\lambda_\theta+2\lambda_\phi}{3+\lambda_\theta}$. The new observable F_1 is rotation invariant in the production plane. The condition that the spin-quantization axis is in the production plane is, indeed, fulfilled in the HX, Collins-Soper, Gottfried-Jackson, and target frames. From Ref. [36], we know that the rotation-invariant property of F_1 is guaranteed from a relation of the Wigner

functions $d_{1,M}^1(\theta) + d_{-1,M}^1(\theta) = \delta_{|M|,1}$. In the section, we want to generalize the relation to the arbitrary spin- n (n is an integer) particles. We straightforwardly write down the linear identities for the Wigner functions:

$$\begin{aligned}
&\sum_{m=-k}^k \langle k, m; k, m | 2k, 2m \rangle d_{2m,M}^{2k}(\theta) \\
&= \langle k, \frac{M}{2}; k, \frac{M}{2} | 2k, M \rangle \delta_{\text{mod}(M,2),0}, \quad n = 2k, \\
&\sum_{m=0}^k \langle 2k+1-m, 0; m, 0 | 2k+1, 0 \rangle \\
&\quad (d_{2k+1-m,M}^{2k+1}(\theta) + d_{m-2k-1,M}^{2k+1}(\theta)) \\
&= \langle \frac{|M|+1}{2} + k, 0; \frac{1-|M|}{2} + k, 0 | 2k+1, 0 \rangle \\
&\quad \delta_{\text{mod}(M,2),1}, \quad n = 2k+1, \quad (20)
\end{aligned}$$

where k is a non-negative integer. The amplitudes with respect to a chosen polarization axis can be symbolically denoted as $|n\rangle = \sum_{m=-n}^n a_m |n, m\rangle$, where $|n, m\rangle$ is a J_z eigenstate with the eigenvalues $m = -n, -n+1, \dots, n$, and a_m is the production amplitude, i.e., $\rho_{J_z, J'_z} \equiv \langle a_{J_z} a_{J'_z}^* \rangle$ (average over the events, assuming that for each event the particle can be produced in a different angular momentum state). From Eq.(20), we can immediately draw a conclusion that the linear combinations of amplitudes

$$b_{2k} \equiv \sum_{m=-k}^k \langle k, m; k, m | 2k, 2m \rangle a_{2m}, \text{ when } n = 2k,$$

and

$$\begin{aligned}
b_{2k+1} &\equiv \sum_{m=0}^k \langle 2k+1-m, 0; m, 0 | 2k+1, 0 \rangle \\
&\quad (a_{2k+1-m} + a_{m-2k-1}), \text{ when } n = 2k+1,
\end{aligned}$$

are invariant under the rotation in the production plane. Therefore, the observables like F_n defined as

$$\begin{aligned}
F_n &\equiv \frac{1}{B_n} \frac{\langle |b_n|^2 \rangle}{N_n}, \\
N_n &\equiv \sum_{m=-n}^n \langle |a_m|^2 \rangle \equiv \sum_{m=-n}^n \rho_{m,m}, \quad (21)
\end{aligned}$$

are rotation-invariant, where B_n is a normalization factor to ensure $0 \leq F_n \leq 1$. In a more extended sense, any function of F_n is rotation-invariant. F_n can be expressed in terms of the coefficients of the decay angular distribution (e.g., $\lambda_\theta, \lambda_\phi$, etc). Specifically, for the spin-1 particles, the observable is

$$F_1 \equiv \frac{1}{2} \frac{\langle |a_1 + a_{-1}|^2 \rangle}{\langle |a_1|^2 + |a_0|^2 + |a_{-1}|^2 \rangle}, \quad (22)$$

while for the spin-2 particles, its expression is

$$F_2 \equiv \frac{1}{3} \frac{\langle |a_2 + \sqrt{\frac{2}{3}}a_0 + a_{-2}|^2 \rangle}{\langle |a_2|^2 + |a_1|^2 + |a_0|^2 + |a_{-1}|^2 + |a_{-2}|^2 \rangle}. \quad (23)$$

As examples of F_1 , we consider the J/ψ decay into two muons and the χ_{c1} decay into a J/ψ and a photon. For the J/ψ ,⁴

$$F_1^{J/\psi \rightarrow \mu^+ \mu^-} = \frac{1 + \lambda_{\theta'} + 2\lambda_{\phi'}}{3 + \lambda_{\theta'}}, \quad (24)$$

which has been presented in Ref. [36], while for the χ_{c1} , one can derive

$$F_1^{\chi_{c1} \rightarrow J/\psi \gamma} = \frac{1 - \lambda_{\theta} - 4\lambda_{\phi}}{3 + \lambda_{\theta}} \quad (25)$$

from Eqs.(8) and (22).⁵ The χ_{c2} provides an example of the spin-2 particles. In fact, the complete angular distribution of the χ_{c2} 's decay product J/ψ is Eq.(D3) instead of Eq.(11). However, the terms absent in Eq.(11) are suppressed, as mentioned above. Hence, the spin information in Eq.(12) is not sufficient. In Appendix B, we have included the E1,M2, and E3 effects into the angular distribution of J/ψ in $\chi_{c2} \rightarrow J/\psi \gamma$ and derived the $F_2^{\chi_{c2} \rightarrow J/\psi \gamma}$ there [see Eq.(B6)]. We suggest that the reader who is interested in this part to refer to Appendix B. These frame-invariant relations can be extended to the study of other bosons or mesons. The experimentalists can measure these observables to make a cross-check of their extractions of the angular distribution coefficients in different frames.

VII. UNCERTAINTY OF J/ψ POLARIZATION FROM FEED-DOWN

The CDF data for the prompt- J/ψ production include not only direct- J/ψ production but also the feed-down contributions from χ_{cJ} and ψ' . However, the recent NLO calculations of J/ψ polarization in Refs. [18, 19] are devoid of the feed-down contributions. Though the LO NRQCD prediction of the feed down to the J/ψ polarization in Ref. [37] was found to have a minor impact on

the final LO result, one may still doubt whether the NLO feed-down effect on $\lambda_{\theta'}$ ⁶ of the J/ψ can be neglected, because the NLO correction to the P wave is large [8]. In this section, we will estimate the possible uncertainty of the J/ψ polarization $\lambda_{\theta'}$ arising from the feed down of the χ_c and ψ' decays.

The calculation of the prompt- J/ψ polarization is complex. In general, prompt data are composed of four parts, i.e., the direct production of the J/ψ , the single-cascade decays of the χ_c and of the ψ' , and the double-cascade decay $\psi' \rightarrow \chi_c \gamma \rightarrow J/\psi \gamma \gamma$. The direct production of the J/ψ has been studied, e.g., in Refs. [18, 19]. The relation between the production SDMEs of the χ_c and the SDMEs of the J/ψ from χ_c decays is given by Eq.(19), whereas the relation between the production SDMEs of the ψ' and the SDMEs of the χ_c coming from ψ' decay is

$$\rho_{J_z, J'_z}^{\psi' \rightarrow \chi_{cJ}} \propto \sum_{l_z, s_z, s'_z = \pm 1, 0} \langle 1, l_z; 1, s_z | J, J_z \rangle \langle 1, l_z; 1, s'_z | J, J'_z \rangle \rho_{s_z, s'_z}^{\psi'} \quad (26)$$

By combining Eqs.(27) and (19), the double-cascade decay component can also be calculated. However, in the following uncertainties estimation, we will neglect this contribution, because of the small branching ratio and small cross section ratio between ψ' and J/ψ [13]. Finally, the single-cascade decay $\psi' \rightarrow J/\psi \pi \pi$ can be treated in analogy with the double chromoelectric dipole transition $^3S_1^{[8]} \rightarrow J/\psi$ [37]. This part will also not be included in the uncertainties because of the small cross section ratio between ψ' and J/ψ [13] and the spin orientation conserved in $\psi' \rightarrow J/\psi \pi \pi$ [38].

In this way, the only contribution to be considered is the feed down from χ_c . We consider the total prompt- J/ψ yield ρ decomposed in the “direct” part, ρ^d , already calculated in NRQCD at the NLO level, and the “feed-down” part ρ^f , with their corresponding polarization observables $\lambda_{\theta'}^d$ and $\lambda_{\theta'}^f$, polar anisotropies of the dilepton decay distributions. The fraction of the J/ψ yield from feed down with respect to the total prompt yield is denoted as r , i.e., $r \equiv \frac{2\rho_{1,1}^f + \rho_{0,0}^f}{2\rho_{1,1}^f + \rho_{0,0}^f + 7\rho_{0,0}^d}$ with $\rho_{s_z, s'_z} \equiv \rho_{s_z, s'_z}^f + \rho_{s_z, s'_z}^d$ and $\rho \equiv 2\rho_{1,1} + \rho_{0,0}$. Hence, the prompt- J/ψ decay polar anisotropy is

$$\rho_{0,0}^f = r \frac{1 - \lambda_{\theta'}^f}{3 + \lambda_{\theta'}^f} \rho, \quad \rho_{1,1}^f = r \frac{1 + \lambda_{\theta'}^f}{3 + \lambda_{\theta'}^f} \rho, \quad (27)$$

$$\rho_{0,0}^d = (1 - r) \frac{1 - \lambda_{\theta'}^d}{3 + \lambda_{\theta'}^d} \rho, \quad \rho_{1,1}^d = (1 - r) \frac{1 + \lambda_{\theta'}^d}{3 + \lambda_{\theta'}^d} \rho,$$

⁴ Since the invariants are only defined to be invariant with respect to rotations in the production plane, the invariance of $F_1^{J/\psi \rightarrow \mu^+ \mu^-}$ is satisfied when J/ψ is directly produced or from χ_c decay in the second option but not in the first option. However, in the first option, one can still define invariants with respect to rotations in the χ_c decay plane.

⁵ Note that the expressions of $F_1^{J/\psi \rightarrow \mu^+ \mu^-}$ and $F_1^{\chi_{c1} \rightarrow J/\psi \gamma}$ as functions of the polarization observables λ 's can also be written in one common form being $F_1^{\chi_{c1} \rightarrow J/\psi \gamma} = 1 - 2F_1^{J/\psi \rightarrow \mu^+ \mu^-}$. This fact can also be expected from the rotation relations of λ 's given in Ref. [6].

⁶ Note that, to be consistent throughout the context, the polarization observables of the J/ψ or the angular distributions of the muon are all denoted by an extra prime.

⁷ Note that we use the symmetry property $\rho_{-\lambda, -\lambda'}^H = (-)^{\lambda - \lambda'} \rho_{\lambda, \lambda'}^H$, which is guaranteed in hadroproduction by parity invariance [39].

and

$$\lambda_{\theta'} = \frac{\frac{r\lambda_{\theta'}^f}{3+\lambda_{\theta'}^f} + \frac{(1-r)\lambda_{\theta'}^d}{3+\lambda_{\theta'}^d}}{\frac{r}{3+\lambda_{\theta'}^f} + \frac{1-r}{3+\lambda_{\theta'}^d}}. \quad (28)$$

All these considerations are valid for any polarization frame. From Eq.(18), we know that the J/ψ from χ_{c1} and χ_{c2} can have $-\frac{1}{3} \leq \lambda_{\theta'}^{\chi_{c1}} \leq 1$ and $-\frac{3}{5} \leq \lambda_{\theta'}^{\chi_{c2}} \leq 1$. Therefore, we take the $-\frac{43}{105} \leq \lambda_{\theta'}^f \leq 1$, which is weighted by the relative contributions of χ_{c1} and χ_{c2} to prompt J/ψ , i.e., $\sigma_{\chi_{c1}}\mathcal{B}(\chi_{c1} \rightarrow J/\psi\gamma)/\sigma_{\chi_{c2}}\mathcal{B}(\chi_{c2} \rightarrow J/\psi\gamma) \cong 5 : 2$, as measured by CDF [7]. For example, let us compare the cases $\lambda_{\theta'}^d = 0$ and $\lambda_{\theta'}^d = 1$, approximated values of the direct- J/ψ polarization predictions in the HX frame for $p_T > 10\text{GeV}$ at the Tevatron according to Refs. [18, 19], respectively. The allowed prompt- J/ψ polarization ranges in the two cases (with $\lambda_{\theta'}^f$ varying from $-\frac{43}{105}$ to 1) are $-\frac{129r}{272+43r} \leq \lambda_{\theta'} \leq \frac{3r}{4-r}$ and $\frac{68-111r}{68+37r} \leq \lambda_{\theta'} \leq 1$. If we fix $r = 0.3$ (the central value of the average χ_c feed-down fraction to prompt J/ψ measured at the Tevatron [40]), the feed-down contribution may change $\lambda_{\theta'}$ from 0.24 to -0.14 when $\lambda_{\theta'}^d = 0$ and from 1 to 0.44 when the polarization of the direct J/ψ is fully transverse. More generally, Fig. 1 shows curves for the prompt- J/ψ polarization $\lambda_{\theta'}$ as a function of the direct- J/ψ polarization $\lambda_{\theta'}^d$, for $\lambda_{\theta'}^f = +1, 0, -\frac{43}{105}$, and $r = 0.3$. The upper and lower curves represent physical bounds for $\lambda_{\theta'}$. Figure 2 shows the maximum possible impact of the feed down from the χ_c decays on the prompt- J/ψ polarization predicted in the HX frame for the Tevatron with $\sqrt{s} = 1.96\text{TeV}$ and $|y_{J/\psi}| < 0.6$. The LDMEs values (see Table I) used for the direct- J/ψ prediction are those obtained in Ref. [19] by fitting the NLO NRQCD calculation to the Tevatron data. Only the central value of the direct- J/ψ prediction is shown. In particular, the prediction of an almost unpolarized J/ψ production obtained with the LDMEs determined in Ref. [19] is not drastically affected by the neglected impact of the χ_c feed-down contribution.

TABLE I: CO LDMEs for J/ψ from Ref. [19] obtained by fitting the differential cross section and polarization of prompt J/ψ simultaneously at the Tevatron [5]. The CS LDME is calculated with the B-T potential model in Ref. [41].

$\langle\mathcal{O}^{J/\psi}(^3S_1^{[1]})\rangle$ GeV ³	$\langle\mathcal{O}^{J/\psi}(^1S_0^{[8]})\rangle$ 10 ⁻² GeV ³	$\langle\mathcal{O}^{J/\psi}(^3S_1^{[8]})\rangle$ 10 ⁻² GeV ³	$\langle\mathcal{O}^{J/\psi}(^3P_0^{[8]})\rangle/m_c^2$ 10 ⁻² GeV ³
1.16	8.9	0.30	0.56

VIII. AN EXAMPLE OF χ_{c1} AND χ_{c2} POLARIZATION

In this section, we are in a position to give an example for the inclusive χ_{c1} and χ_{c2} production at the LHC with

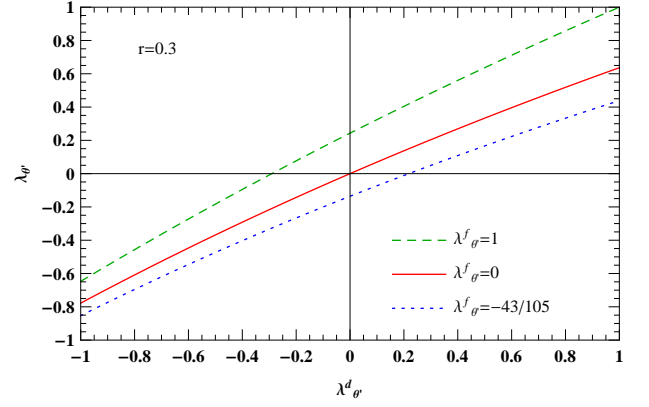


FIG. 1: (color online). Possible impact of the feed down on the prompt- J/ψ polar anisotropy $\lambda_{\theta'}$ as a function of the direct- J/ψ polarization $\lambda_{\theta'}^d$. Here, $r = 0.3$ is assumed, and the curves correspond to J/ψ polarizations from the feed down $\lambda_{\theta'}^f = +1, 0, -\frac{43}{105}$.

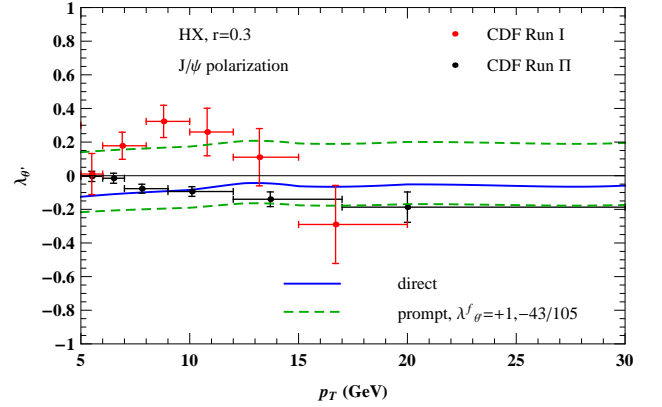


FIG. 2: (color online). The direct- J/ψ polarization $\lambda_{\theta'}$ in the HX frame at the Tevatron calculated with the LDMEs of Table I, and the corresponding upper and lower limits for the prompt- J/ψ polarization assuming the χ_c feed-down contribution $r = 0.3$. CDF data are taken from Refs. [4, 5].

$\sqrt{s} = 8\text{ TeV}$.⁸ We also present the contributions of the individual Fock states to the SDMEs, for the convenience of the readers who want to use our results with different LDME values.

We use our automatic matrix element and event generator HELAC-Onia [42] to calculate all the SDMEs under

⁸ To avoid possible misunderstanding, we want to remind the readers that we only give LO NRQCD results here as a simple application of the formulas presented in the paper. We do not intend to give phenomenological predictions of χ_c polarization. As pointed out in Ref. [8], there is a kinematical enhancement of P wave at NLO, which results in a large cancellation between the P wave and S wave. Our more reliable NLO phenomenological results for χ_c are presented in an independent paper [24].

the relevant conditions. The generator is built on rewritten versions of the published HELAC [43, 44], PHEGAS [45, 46], RAMBO [47], and VEGAS [48] codes. The program has been extensively tested.

The input parameters in our calculations are

- (1) $m_c = 1.5 \text{ GeV}, m_{\chi_c} = 2m_c = 3\text{GeV}$,⁹
- (2) $\sqrt{s} = 8 \text{ TeV}, |y_{\chi_c}| < 2.4$,
- (3) the CTEQ6L1 [49] set of parton distribution functions,
- (4) renormalization and factorization scales $\mu_r = \mu_f = \sqrt{(2m_c)^2 + p_T^2}$,
- (5) CS LDMEs $\langle \mathcal{O}^{\chi_{cJ}}(P_J^{[1]}) \rangle = \frac{3(2J+1)2N_c}{4\pi} |R'_P(0)|^2$, with $|R'_P(0)|^2 = 0.075\text{GeV}^5$ [41], and
- (6) CO LDMEs $\frac{\langle \mathcal{O}^{\chi_{cJ}}(S_1^{[8]}) \rangle}{2J+1} = 2.2 \times 10^{-3}\text{GeV}^3$ [8].

The relations between the SDMEs of $S_1^{[8]}$ and those of ${}^3P_J^{[1]}$ are identical to those in Eq.(27) and are specifically

$$\rho_{J_z, J'_z}^{S_1^{[8]} \rightarrow \chi_{cJ}} \propto \sum_{l_z, s_z, s'_z = \pm 1, 0} \langle 1, l_z; 1, s_z | J, J_z \rangle \langle 1, l_z; 1, s'_z | J, J'_z \rangle \rho_{s_z, s'_z}^{S_1^{[8]}}. \quad (29)$$

The results of the calculations are organized in the following groups of figures, where in each case, from top to bottom, three different polarization frames are considered (HX, Collins-Soper, Gottfried-Jackson): Figs.(3,4,5) show the partial cross sections ($\frac{d\sigma_{00}}{dp_T}, \frac{d\sigma_{11}}{dp_T}, \frac{d\sigma_{22}}{dp_T}$) and the total cross sections ($\frac{d\sigma_{\text{tot}}}{dp_T}$) as a function of p_T for each individual Fock state contributing to χ_c production (${}^3P_1^{[1]}, {}^3P_2^{[1]}$, and $S_1^{[8]}$, with $\frac{d\sigma_{\text{tot}}}{dp_T} = 2\frac{d\sigma_{11}}{dp_T} + \frac{d\sigma_{00}}{dp_T}$ for ${}^3P_1^{[1]}$ and $S_1^{[8]}$, $\frac{d\sigma_{\text{tot}}}{dp_T} = 2\frac{d\sigma_{22}}{dp_T} + 2\frac{d\sigma_{11}}{dp_T} + \frac{d\sigma_{00}}{dp_T}$ for ${}^3P_2^{[1]}$). The corresponding nondiagonal SDMEs are shown in Figs.(6,7,8). The frame-dependent parameters $\lambda_\theta, \lambda_\phi$, and $\lambda_{\theta\phi}$ of the radiative χ_c decays are shown in Figs.(9,10,11) for the χ_{c1} and in Figs.(12,13,14) for the χ_{c2} , with distinct curves for the CS-only result and for the full CS+CO calculation. We remind that these parameters are also identical, in the E1-only approximation, to the parameters $\lambda_{\theta'}, \lambda_{\phi'}$, and $\lambda_{\theta'\phi'}$ of the dilepton distribution of the J/ψ from χ_{c1} decays in the second option, for each considered polarization frame. Finally, Figs.(15) and (16) show the results for the corresponding frame-independent polarization parameters F_1 and F_2 .

Some features should be emphasized:

- (1) From the curves of the total cross sections in Figs.(3,4,5), we may conclude that the CS dominates in the low transverse momentum region, while the CO may dominate when p_T increases because gluon fragmentation processes [50] become important. The CS p_T distribution may receive significant contributions from the higher order radiative corrections [8]. The full NLO predictions for χ_{cJ} polarizations are already presented in Ref. [24].
- (2) The polarization parameters in the Gottfried-Jackson frame tend to be very similar to those in the HX frame, especially at high p_T , while significant differences exist between these two and the Collins-Soper frame. The HX and Collins-Soper frames are, therefore, sufficient for the characterization of the angular distributions. In particular, from Fig.5, we see that the longitudinal cross section of the $S_1^{[8]}$ channel is largest in the Collins-Soper frame when $p_T \gg 2m_c$, in agreement with the statement in Ref. [22].
- (3) We have verified that the results of $\rho_{i,j}$ in the Gottfried-Jackson frame and the target frame coincide within error bars, aside from a factor $(-1)^{i-j}$, which is also pointed out in Ref. [22]. Therefore, we will not present the results in the target frame here. For diagonal elements, i.e., $\rho_{i,i}$, the curves in the Gottfried-Jackson are similar to those in the helicity frame and different from those in the Collins-Soper frame. Hence, for the polarization observable λ_θ , the helicity and the Collins-Soper frames are enough. Moreover, from Fig.(5), we see that the longitudinal cross section of the $S_1^{[8]}$ channel is the largest in the Collins-Soper frame when $p_T \gg 2m_c$, which is consistent with the statement in Ref. [27].
- (4) In the HX and the Collins-Soper frames, the SDMEs $\rho_{i,j}$ with $|i-j|$ odd are almost zero. Therefore, they should be measured in the Gottfried-Jackson frame as well as $\lambda_{\theta\phi}$ and $\lambda_{\theta'\phi'}$ shown in Figs.(11) and (14). In fact, this is a consequence of the definition of the Y axis taken always as $P_1 \times (-P_2)$ (in the χ_c rest frame) both at positive and negative rapidity. Actually, the values of $\lambda_{\theta\phi}$ in the positive and negative rapidity are opposite. The existence of these relations between the choice of the Y axis and the sign $\lambda_{\theta\phi}$ was already pointed out in Ref. [6]. On the other hand, for $\rho_{i,j}$ with $|i-j|$ even, the measurements in the HX and the Collins-Soper frames are more significant than in the Gottfried-Jackson frame.
- (5) The frame-independent observables defined in Eqs.(22) and (23) for the χ_{c1} and the χ_{c2} are shown in Fig.15. The figures show the frame-independent property of $F_1^{\chi_{c1} \rightarrow J/\psi \gamma}$ and $F_2^{\chi_{c2} \rightarrow J/\psi \gamma}$ by direct numerical calculation. Hence, it would be interesting to measure these observables at the LHC. In

⁹ We use the approximation $m_{\chi_c} = m_{J/\psi} = 2m_c$ here. The mass dependences of the result is mild when $p_T^{\chi_c} \simeq p_T^{J/\psi} > 2m_c$.

particular, it is remarkable that $F_2^{\chi_{c2} \rightarrow J/\psi \gamma}$ is practically independent of p_T , contrary to λ_θ and λ_ϕ in all frames considered (see Figs.(12) and (13)).

IX. SUMMARY

Finally, we draw our conclusion. The upgrade of the integrated luminosity at the LHC will not only allow us to measure the polarizations of S -wave quarkonium states like J/ψ and ψ' but also the angular distributions of decay products from the P -wave states χ_{cJ} . This opens new opportunities to further test NRQCD factorization and the quarkonium production mechanisms, in general. We have presented a general calculation framework based on the shape of the decay vertex functions to investigate the polarizations of the χ_{cJ} states and their impact in the observed prompt- J/ψ polarization. We have derived general expressions for the polar and azimuthal angle distributions of the χ_{c1} and χ_{c2} decays into $J/\psi \gamma$ and for the subsequent J/ψ decay into muons. The coefficients of the angular distributions have been calculated as a function of the χ_c production SDMEs [Eqs.(8), (12), (14), (18), and (D4)]. We have derived rotation-invariant relations for arbitrary integer-spin particles [Eq.(21)] and in the specific cases of χ_{c1} and χ_{c2} decays. As an example of an application of our calculation framework, in the NRQCD factorization, we have calculated the tree-level angular distributions of the χ_{c1} and χ_{c2} decays at the LHC considering several polarization frames and also frame-independent quantities. Moreover, we have also estimated the impact of the χ_c feed down in the polarization of prompt J/ψ . We found that our previous direct- J/ψ polarization results [19] will not change much after including this part. A more detailed phenomenological analysis of the yields and polarizations of χ_c in hadroproduction are performed in Ref. [24], based on our complete NLO NRQCD calculations.

Note added: While this paper was prepared, a new preprint [51] for polarizations of the prompt- J/ψ and ψ' production at the LHC and Tevatron appeared. The authors extracted a set of CO LDMEs for the J/ψ other than those in Refs. [18, 19] by including the χ_{cJ} and ψ' feed-down contributions. Their LDMEs result in two combinations of LDMEs that agree with those extracted in Refs. [13, 19], and their prompt polarization result is around the upper limit in Fig.2 of this paper.

Acknowledgments

We thank J.-P. Lansberg, Q.-H. Cao and Y.-Q. Ma for helpful discussions. This work was supported in part by the National Natural Science Foundation of China (Grants No.11021092 and No.11075002) and the Ministry of Science and Technology of China (Grant No.2009CB825200).

Appendix A: Decay angular distribution of spin-1 bosons

The most general expression for the decay angular distribution of a vector boson V without assuming parity conservation is

$$\begin{aligned} \mathcal{W}^V(\theta, \phi) \propto & 1 + \lambda_\theta \cos^2 \theta + \lambda_\phi \sin^2 \theta \cos \phi \\ & + \lambda_{\theta\phi} \sin 2\theta \cos \phi + \lambda_\phi^\perp \sin^2 \theta \sin 2\phi \\ & + \lambda_{\theta\phi}^\perp \sin 2\theta \sin \phi + 2\eta_\theta \cos \theta \\ & + 2\eta_{\theta\phi} \sin \theta \cos \phi + 2\eta_{\theta\phi}^\perp \sin \theta \sin \phi, \quad (\text{A1}) \end{aligned}$$

with

$$\begin{aligned} \lambda_\theta &= (1 - 3\delta) \frac{N_V - 3\rho_{0,0}^V}{(1 + \delta)N_V + (1 - 3\delta)\rho_{0,0}^V}, \\ \lambda_\phi &= (1 - 3\delta) \frac{2\Re\rho_{1,-1}^V}{(1 + \delta)N_V + (1 - 3\delta)\rho_{0,0}^V}, \\ \lambda_{\theta\phi} &= (1 - 3\delta) \frac{\sqrt{2}(\Re\rho_{1,0}^V - \Re\rho_{-1,0}^V)}{(1 + \delta)N_V + (1 - 3\delta)\rho_{0,0}^V}, \\ \lambda_\phi^\perp &= -(1 - 3\delta) \frac{2\Im\rho_{1,-1}^V}{(1 + \delta)N_V + (1 - 3\delta)\rho_{0,0}^V}, \\ \lambda_{\theta\phi}^\perp &= -(1 - 3\delta) \frac{\sqrt{2}(\Im\rho_{1,0}^V + \Im\rho_{-1,0}^V)}{(1 + \delta)N_V + (1 - 3\delta)\rho_{0,0}^V}, \\ \eta_\theta &= \alpha \frac{\rho_{1,1}^V - \rho_{-1,-1}^V}{(1 + \delta)N_V + (1 - 3\delta)\rho_{0,0}^V}, \\ \eta_{\theta\phi} &= \alpha \frac{\sqrt{2}(\Re\rho_{1,0}^V + \Re\rho_{-1,0}^V)}{(1 + \delta)N_V + (1 - 3\delta)\rho_{0,0}^V}, \\ \eta_{\theta\phi}^\perp &= -\alpha \frac{\sqrt{2}(\Im\rho_{1,0}^V - \Im\rho_{-1,0}^V)}{(1 + \delta)N_V + (1 - 3\delta)\rho_{0,0}^V}, \quad (\text{A2}) \end{aligned}$$

where $N_V = \rho_{1,1}^V + \rho_{0,0}^V + \rho_{-1,-1}^V$, and the parameters α, δ depend on the identity of V and of its decay products. In particular, α is induced by the parity-violating interactions in the decay. In other words, it is nonzero only when the decay is not a parity conservative process. For the J/ψ decays into dilepton, $\alpha = 0, \delta = 0$, whereas for the pure E1 radiative transition $\chi_{c1} \rightarrow J/\psi \gamma$, $\alpha = 0, \delta = \frac{1}{2}$. If one also wants to include the M2 transition in the χ_{c1} decay, δ should be changed to $\frac{1+2a_1^{J=1}a_2^{J=1}}{2}$, where $a_1^{J=1}, a_2^{J=1}$ represent the E1 and M2 amplitudes, respectively, with the normalization $(a_1^{J=1})^2 + (a_2^{J=1})^2 = 1$. They have been measured in Refs. [29, 30, 32]. The numerical values measured are shown in Table II. Without losing generality, the rotation-invariant observable F_1 de-

fixed in Eq.(22) can be written as¹⁰

$$F_1 = \frac{1 - 3\delta + (1 - \delta)\lambda_\theta + 2\lambda_\phi}{(1 - 3\delta)(3 + \lambda_\theta)}. \quad (\text{A3})$$

TABLE II: The normalized M2 amplitude $a_2^{J=1}$ for $\chi_{c1} \rightarrow J/\psi\gamma$ as measured by different experiments.

Experiment	$a_2^{J=1}(10^{-2})$
CLEO [29]	$-6.26 \pm 0.63 \pm 0.24$
Crystal Ball [30]	$-0.2^{+0.8}_{-2.0}$
E835 [32]	$0.2 \pm 3.2 \pm 0.4$

In order to show the impact of the higher-order multipole M2 contribution to the χ_{c1} polarizations, we take the example illustrated in Sec. VII. As an illustrative case, only λ_θ in the HX frame is shown in Fig. 17, where E1 means pure E1 transtion approximation and E1+M2 means that we have included the full E1 and M2 transitions using the CLEO [29] measured $a^{J=1}$ in Table II.

Appendix B: Decay angular distribution of spin-2 bosons

The general decay angular distributions of spin-2 tensor particles T can have up to 24 observable parameters:

$$\begin{aligned} \mathcal{W}^T(\theta, \phi) \propto & 1 + \lambda_\theta \cos^2 \theta + \lambda_{2\theta} \cos^4 \theta \\ & + \lambda_{\theta\phi} \sin 2\theta \cos \phi + \lambda_{2\theta\phi} \sin 2\theta \sin^2 \theta \cos \phi \\ & + \lambda_{\theta\phi}^\perp \sin 2\theta \sin \phi + \lambda_{2\theta\phi}^\perp \sin 2\theta \sin^2 \theta \sin \phi \\ & + \lambda_\phi \sin^2 \theta \cos 2\phi + \lambda_{2\phi} \sin^4 \theta \cos 2\phi \\ & + \lambda_\phi^\perp \sin^2 \theta \sin 2\phi + \lambda_{2\phi}^\perp \sin^4 \theta \sin 2\phi \\ & + \lambda_{3\theta\phi} \sin 2\theta \sin^2 \theta \cos 3\phi \\ & + \lambda_{3\theta\phi}^\perp \sin 2\theta \sin^2 \theta \sin 3\phi \\ & + \lambda_{4\phi} \sin^4 \theta \cos 4\phi + \lambda_{4\phi}^\perp \sin^4 \theta \sin 4\phi \\ & + 2\eta_\theta \cos \theta + 2\eta_{2\theta} \cos^3 \theta \\ & + 2\eta_{\theta\phi} \sin \theta \cos \phi + 2\eta_{2\theta\phi} \sin^3 \theta \cos \phi \\ & + 2\eta_{\theta\phi}^\perp \sin \theta \sin \phi + 2\eta_{2\theta\phi}^\perp \sin^3 \theta \sin \phi \\ & + 2\eta_\phi \sin^2 \theta \cos \theta \cos 2\phi + 2\eta_\phi^\perp \sin^2 \theta \cos \theta \sin 2\phi \\ & + 2\eta_{3\theta\phi} \sin^3 \theta \cos 3\phi \\ & + 2\eta_{3\theta\phi}^\perp \sin^3 \theta \sin 3\phi, \end{aligned} \quad (\text{B1})$$

where

$$\begin{aligned} \lambda_\theta &= 6[(1 - 3\delta_0 - \delta_1)N_T \\ &\quad - (1 - 7\delta_0 + \delta_1)(\rho_{1,1}^T + \rho_{-1,-1}^T) \\ &\quad - (3 - \delta_0 - 7\delta_1)\rho_{0,0}^T]/R, \\ \lambda_{2\theta} &= (1 + 5\delta_0 - 5\delta_1)[N_T - 5(\rho_{1,1}^T + \rho_{-1,-1}^T) \\ &\quad + 5\rho_{0,0}^T]/R, \\ \lambda_{\theta\phi} &= 4[2(1 - \delta_0 - 2\delta_1)(\Re\rho_{2,1}^T - \Re\rho_{-2,-1}^T) \\ &\quad - \sqrt{6}(2\delta_0 - \delta_1)(\Re\rho_{1,0}^T - \Re\rho_{-1,0}^T)]/R, \\ \lambda_{2\theta\phi} &= -2(1 + 5\delta_0 - 5\delta_1)[(\Re\rho_{2,1}^T - \Re\rho_{-2,-1}^T) \\ &\quad - \sqrt{6}(\Re\rho_{1,0}^T - \Re\rho_{-1,0}^T)]/R, \\ \lambda_{\theta\phi}^\perp &= 4[-2(1 - \delta_0 - 2\delta_1)(\Im\rho_{2,1}^T + \Im\rho_{-2,-1}^T) \\ &\quad + \sqrt{6}(2\delta_0 - \delta_1)(\Im\rho_{1,0}^T + \Im\rho_{-1,0}^T)]/R, \\ \lambda_{2\theta\phi}^\perp &= 2(1 + 5\delta_0 - 5\delta_1)[(\Im\rho_{2,1}^T + \Im\rho_{-2,-1}^T) \\ &\quad - \sqrt{6}(\Im\rho_{1,0}^T + \Im\rho_{-1,0}^T)]/R, \\ \lambda_\phi &= 4[\sqrt{6}(1 + \delta_0 - 3\delta_1)(\Re\rho_{2,0}^T + \Re\rho_{-2,0}^T) \\ &\quad - 6(2\delta_0 - \delta_1)\Re\rho_{1,-1}^T]/R, \\ \lambda_{2\phi} &= -2(1 + 5\delta_0 - 5\delta_1)[\sqrt{6}(\Re\rho_{2,0}^T + \Re\rho_{-2,0}^T) \\ &\quad - 4\Re\rho_{1,-1}^T]/R, \\ \lambda_\phi^\perp &= -4[\sqrt{6}(1 + \delta_0 - 3\delta_1)(\Im\rho_{2,0}^T - \Im\rho_{-2,0}^T) \\ &\quad - 6(2\delta_0 - \delta_1)\Im\rho_{1,-1}^T]/R, \\ \lambda_{2\phi}^\perp &= 2(1 + 5\delta_0 - 5\delta_1)[\sqrt{6}(\Im\rho_{2,0}^T - \Im\rho_{-2,0}^T) \\ &\quad - 4\Im\rho_{1,-1}^T]/R, \\ \lambda_{3\theta\phi} &= 2(1 + 5\delta_0 - 5\delta_1)\frac{\Re\rho_{2,-1}^T - \Re\rho_{-2,1}^T}{R}, \\ \lambda_{3\theta\phi}^\perp &= -2(1 + 5\delta_0 - 5\delta_1)\frac{\Im\rho_{2,-1}^T + \Im\rho_{-2,1}^T}{R}, \\ \lambda_{4\phi} &= 2(1 + 5\delta_0 - 5\delta_1)\frac{\Re\rho_{2,-2}^T}{R}, \\ \lambda_{4\phi}^\perp &= -2(1 + 5\delta_0 - 5\delta_1)\frac{\Im\rho_{2,-2}^T}{R}, \end{aligned} \quad (\text{B2})$$

¹⁰ One just substitutes Eq.(A2) into Eq.(22) to get the following expression. We want to remind the readers that because the rotation-invariant observable is not uniquely defined, a more general form of the rotation-invariant observable is an arbitrary function of F_1 .

and

$$\begin{aligned}
\eta_\theta &= 2[(2\alpha_1 + \alpha_2)(\rho_{2,2}^T - \rho_{-2,-2}^T) \\
&\quad - 2(\alpha_1 - \alpha_2)(\rho_{1,1}^T - \rho_{-1,-1}^T)]/R, \\
\eta_{2\theta} &= -2(2\alpha_1 - \alpha_2)[(\rho_{2,2}^T - \rho_{-2,-2}^T) \\
&\quad - 2(\rho_{1,1}^T - \rho_{-1,-1}^T)]/R, \\
\eta_{\theta\phi} &= -4[2(\alpha_1 - \alpha_2)(\Re\rho_{2,1}^T + \Re\rho_{-2,-1}^T) \\
&\quad - \sqrt{6}\alpha_1(\Re\rho_{1,0}^T + \Re\rho_{-1,0}^T)]/R, \\
\eta_{2\theta\phi} &= 2(2\alpha_1 - \alpha_2)[3(\Re\rho_{2,1}^T + \Re\rho_{-2,-1}^T) \\
&\quad - \sqrt{6}(\Re\rho_{1,0}^T + \Re\rho_{-1,0}^T)]/R, \\
\eta_{\theta\phi}^\perp &= 4[2(\alpha_1 - \alpha_2)(\Im\rho_{2,1}^T - \Im\rho_{-2,-1}^T) \\
&\quad - \sqrt{6}\alpha_1(\Im\rho_{1,0}^T - \Im\rho_{-1,0}^T)]/R, \\
\eta_{2\theta\phi}^\perp &= -2(2\alpha_1 - \alpha_2)[3(\Im\rho_{2,1}^T - \Im\rho_{-2,-1}^T) \\
&\quad - \sqrt{6}(\Im\rho_{1,0}^T - \Im\rho_{-1,0}^T)]/R, \\
\eta_\phi &= -2\sqrt{6}(2\alpha_1 - \alpha_2)\frac{\Re\rho_{2,0}^T - \Re\rho_{-2,0}^T}{R}, \\
\eta_\phi^\perp &= 2\sqrt{6}(2\alpha_1 - \alpha_2)\frac{\Im\rho_{2,0}^T + \Im\rho_{-2,0}^T}{R}, \\
\eta_{3\theta\phi} &= -2(2\alpha_1 - \alpha_2)\frac{\Re\rho_{2,-1}^T + \Re\rho_{-2,1}^T}{R}, \\
\eta_{3\theta\phi}^\perp &= 2(2\alpha_1 - \alpha_2)\frac{\Im\rho_{2,-1}^T - \Im\rho_{-2,1}^T}{R}, \tag{B3}
\end{aligned}$$

with

$$\begin{aligned}
N_T &= \rho_{2,2}^T + \rho_{1,1}^T + \rho_{0,0}^T + \rho_{-1,-1}^T + \rho_{-2,-2}^T, \\
R &= (1 + 5\delta_0 + 3\delta_1)N_T \\
&\quad + 3(1 - 3\delta_0 - \delta_1)(\rho_{1,1}^T + \rho_{-1,-1}^T) \\
&\quad + (5 - 7\delta_0 - 9\delta_1)\rho_{0,0}^T. \tag{B4}
\end{aligned}$$

The parameters α_1 and α_2 vanish when parity is conserved, as in the χ_{c2} decay. Other two parameters δ_0 and δ_1 can be determined from the specific processes considered. For the χ_{c2} decays into a J/ψ and a photon, through pure E1 transition, $\delta_0 = \frac{1}{10}$ and $\delta_1 = \frac{3}{10}$, while after including the higher-order multipole amplitudes in the radiative transitions, the coefficients δ_0 and δ_1 can be expressed as the following polynomials in the E1, M2, and E3 amplitudes $a_1^{J=2}, a_2^{J=2}, a_3^{J=2}$:

$$\begin{aligned}
\delta_0 &= [1 + 2a_1^{J=2}(\sqrt{5}a_2^{J=2} + 2a_3^{J=2}) \\
&\quad + 4a_2^{J=2}(a_2^{J=2} + \sqrt{5}a_3^{J=2}) + 3(a_3^{J=2})^2]/10, \\
\delta_1 &= [9 + 6a_1^{J=2}(\sqrt{5}a_2^{J=2} - 4a_3^{J=2}) \\
&\quad - 4a_2^{J=2}(a_2^{J=2} + 2\sqrt{5}a_3^{J=2}) + 7(a_3^{J=2})^2]/30. \tag{B5}
\end{aligned}$$

Again, the normalization of $(a_1^{J=2})^2 + (a_2^{J=2})^2 + (a_3^{J=2})^2 = 1$ has been imposed. The measurements of the multipole amplitudes Refs. [29–32] are listed in Table III. Finally, the expression of the frame-independent parameter F_2 in

terms of the coefficients in Eq.(B1):

$$\begin{aligned}
F_2 &= \frac{n_1 + n_2\lambda_\theta + n_3\lambda_{2\theta} + n_4\lambda_\phi + n_5\lambda_{2\phi} + n_6\lambda_{4\phi}}{d_1 + d_2\lambda_\theta + d_3\lambda_{2\theta}}, \\
n_1 &= \frac{1}{6}, \\
n_2 &= \frac{4 - 4\delta_0 - 3\delta_1}{18(2 - 4\delta_0 - 3\delta_1)}, \\
n_3 &= \frac{2 + 2\delta_0 - 7\delta_1 - 4\delta_0^2 + \delta_0\delta_1 + 3\delta_1^2}{6(1 + 5\delta_0 - 5\delta_1)(2 - 4\delta_0 - 3\delta_1)}, \\
n_4 &= \frac{1}{3(2 - 4\delta_0 - 3\delta_1)}, \\
n_5 &= \frac{2\delta_0 - \delta_1}{(1 + 5\delta_0 - 5\delta_1)(2 - 4\delta_0 - 3\delta_1)}, \\
n_6 &= \frac{1}{1 + 5\delta_0 - 5\delta_1}, \\
d_1 &= \frac{15}{16}, d_2 = \frac{5}{16}, d_3 = \frac{3}{16}. \tag{B6}
\end{aligned}$$

TABLE III: The normalized M2 and E3 amplitudes $a_2^{J=2}, a_3^{J=2}$ for $\chi_{c2} \rightarrow J/\psi\gamma$ as measured by various experiments.

Experiment	$a_2^{J=2}(10^{-2})$	$a_3^{J=2}(10^{-2})$
CLEO(Fit 1) [29]	$-9.3 \pm 1.6 \pm 0.3$	0(fixed)
CLEO(Fit 2) [29]	$-7.9 \pm 1.9 \pm 0.3$	$1.7 \pm 1.4 \pm 0.3$
Crystal Ball [30]	$-33.3^{+11.6}_{-29.2}$	0(fixed)
E760(Fit 1) [31]	-14 ± 6	0(fixed)
E760(Fit 2) [31]	-14^{+8}_{-7}	0^{+6}_{-5}
E835(Fit 1) [32]	$-9.3^{+3.9}_{-4.1} \pm 0.6$	0(fixed)
E835(Fit 2) [32]	$-7.6^{+5.4}_{-5.0} \pm 0.9$	$2.0^{+5.5}_{-4.4} \pm 0.9$

In order to show the impact of the higher-order multipole M2 contribution¹¹ to the χ_{c2} polarizations, we take the example illustrated in Sec. VII as well. As an illustrative example, only λ_θ in the HX frame is illustrated in Fig. 18, where E1 means pure E1 transition approximation and E1+M2 means that we have included the full E1 and M2 transitions, with $a_2^{J=2}$ as measured by the CLEO collaboration [29] (Table III).

Appendix C: Dilepton angular distribution in χ_c decay with multipole effects

We consider here the general expression of the dilepton angular distribution in the decays $\chi_c \rightarrow J/\psi\gamma \rightarrow \mu^+\mu^-\gamma$, including also the higher-order multipole transitions neglected in Sec. V.

In the first option discussed in Sec. V for the definition of the J/ψ quantization axis, the SDMEs for the

¹¹ The E3 amplitude for the χ_{c2} decay is zero from the consideration of the single quark radiation hypothesis.

J/ψ from χ_c decays can be expressed in terms of the χ_c production matrix elements as¹²

$$\begin{aligned} & \rho_{s_z, s'_z}^{\chi_{cJ} \rightarrow J/\psi\gamma} \\ &= \frac{1}{8\pi} \sum_{l=1}^{J+1} \sum_{\lambda_\gamma=\pm l} \int d\Omega [\theta, \phi] \rho_{J_z, J'_z}^{\chi_{cJ}} \mathcal{D}_{J_z, J_{1z}}^{J*} \mathcal{D}_{J'_z, J_{2z}}^J \\ & \langle l, \lambda_\gamma; 1, s_z | J, J_{1z} \rangle \langle J, J_{2z} | 1, \lambda_\gamma; 1, s'_z \rangle \\ & (2l+1)(a_l^{J=J})^2 \text{Br}(\chi_{cJ} \rightarrow J/\psi\gamma). \end{aligned} \quad (\text{C1})$$

The coefficients are expressed as

$$\begin{aligned} \lambda_{\theta'}^{\chi_{c1}} &= -\frac{1-3(a_2^{J=1})^2}{3-(a_2^{J=1})^2}, \lambda_{\phi'}^{\chi_{c1}} = \lambda_{\phi'}^{\perp\chi_{c1}} = 0, \\ \lambda_{\theta'\phi'}^{\chi_{c1}} &= \frac{\sqrt{2}(a_1^{J=1})^2(\Re(\rho_{1,0}^{\chi_{c1}}) - \Re(\rho_{-1,0}^{\chi_{c1}}))}{4(3-(a_2^{J=1})^2)N_{\chi_{c1}}}, \\ \lambda_{\theta'\phi'}^{\perp\chi_{c1}} &= -\frac{\sqrt{2}(a_1^{J=1})^2(\Im(\rho_{1,0}^{\chi_{c1}}) + \Im(\rho_{-1,0}^{\chi_{c1}}))}{4(3-(a_2^{J=1})^2)N_{\chi_{c1}}}, \\ \lambda_{\theta'}^{\chi_{c2}} &= \frac{3(1-11(a_2^{J=2})^2+9(a_3^{J=2})^2)}{39+11(a_2^{J=2})^2-9(a_3^{J=2})^2}, \\ \lambda_{\phi'}^{\chi_{c2}} &= \frac{(a_1^{J=2})^2(7\sqrt{6}(\Re\rho_{0,2}^{\chi_{c2}} + \Re\rho_{0,-2}^{\chi_{c2}}) + 12\Re\rho_{1,-1}^{\chi_{c2}})}{2(39+11(a_2^{J=2})^2-9(a_3^{J=2})^2)N_{\chi_{c2}}}, \\ \lambda_{\theta'\phi'}^{\chi_{c2}} &= [\sqrt{6}(1-\frac{13}{3}(a_2^{J=2})^2-(a_3^{J=2})^2)(\Re\rho_{-1,0}^{\chi_{c2}} - \Re\rho_{1,0}^{\chi_{c2}}) \\ & + 6(4-9(a_2^{J=2})^2-4(a_3^{J=2})^2)(\Re\rho_{-2,-1}^{\chi_{c2}} - \Re\rho_{2,1}^{\chi_{c2}})] \\ & / [4(39+11(a_2^{J=2})^2-9(a_3^{J=2})^2)N_{\chi_{c2}}], \\ \lambda_{\phi'}^{\perp\chi_{c2}} &= \frac{(a_1^{J=2})^2(7\sqrt{6}(\Im\rho_{0,2}^{\chi_{c2}} - \Im\rho_{0,-2}^{\chi_{c2}}) - 12\Im\rho_{1,-1}^{\chi_{c2}})}{2(39+11(a_2^{J=2})^2-9(a_3^{J=2})^2)N_{\chi_{c2}}}, \\ \lambda_{\theta'\phi'}^{\perp\chi_{c2}} &= [\sqrt{6}(1-\frac{13}{3}(a_2^{J=2})^2-(a_3^{J=2})^2)(\Im\rho_{-1,0}^{\chi_{c2}} + \Im\rho_{1,0}^{\chi_{c2}}) \\ & + 6(4-9(a_2^{J=2})^2-4(a_3^{J=2})^2)(\Im\rho_{-2,-1}^{\chi_{c2}} + \Im\rho_{2,1}^{\chi_{c2}})] \\ & / [4(39+11(a_2^{J=2})^2-9(a_3^{J=2})^2)N_{\chi_{c2}}]. \end{aligned}$$

As remarked previously, some of the polarization observables are trivial and devoid of spin information. However, these observables can, in principle, be measured to extract the multipole amplitudes of the χ_c decay, for example, in electron-positron collisions.

In the second option, in which the quantization axis for the $J/\psi \rightarrow \mu^+\mu^-$ decay coincides with the χ_c quantization axis, the general relation between the SDMEs of the $\chi_{cJ} \rho_{J_z, J'_z}^{\chi_{cJ}}$ and those of the J/ψ from the χ_{cJ} decay

$\rho_{s_z, s'_z}^{\chi_{cJ} \rightarrow J/\psi\gamma}$ in the full multipole expansion is

$$\begin{aligned} \rho_{s_z, s'_z}^{\chi_{cJ} \rightarrow J/\psi\gamma} &\propto \sum_{l=1}^{J+1} \sum_{l_z=-l}^l \sum_{J_z, J'_z} (a_l^{J=J})^2 \langle l, l_z; 1, s_z | J, J_z \rangle \\ &\langle J, J'_z | l, l_z; 1, s'_z \rangle \rho_{J_z, J'_z}^{\chi_{cJ}} \text{Br}(\chi_{cJ} \rightarrow J/\psi\gamma). \end{aligned} \quad (\text{C2})$$

The coefficients of the μ^+ angular distribution are

$$\begin{aligned} \lambda_{\theta'}^{\chi_{c1}} &= \frac{-N_{\chi_{c1}} + 3\rho_{0,0}^{\chi_{c1}}}{R_1}, \\ \lambda_{\phi'}^{\chi_{c1}} &= -\frac{2\Re\rho_{1,-1}^{\chi_{c1}}}{R_1}, \\ \lambda_{\theta'\phi'}^{\chi_{c1}} &= -\frac{\sqrt{2}(\Re\rho_{1,0}^{\chi_{c1}} - \Re\rho_{-1,0}^{\chi_{c1}})}{R_1}, \\ \lambda_{\phi'}^{\perp\chi_{c1}} &= \frac{2\Im\rho_{1,-1}^{\chi_{c1}}}{R_1}, \\ \lambda_{\theta'\phi'}^{\perp\chi_{c1}} &= \frac{\sqrt{2}(\Im\rho_{1,0}^{\chi_{c1}} + \Im\rho_{-1,0}^{\chi_{c1}})}{R_1}, \\ \lambda_{\theta'}^{\chi_{c2}} &= \frac{6N_{\chi_{c2}} - 9(\rho_{1,1}^{\chi_{c2}} + \rho_{-1,-1}^{\chi_{c2}}) - 12\rho_{0,0}^{\chi_{c2}}}{R_2}, \\ \lambda_{\phi'}^{\chi_{c2}} &= \frac{2\sqrt{6}(\Re\rho_{2,0}^{\chi_{c2}} + \Re\rho_{-2,0}^{\chi_{c2}}) + 6\Re\rho_{1,-1}^{\chi_{c2}}}{R_2}, \\ \lambda_{\theta'\phi'}^{\chi_{c2}} &= \frac{6(\Re\rho_{2,1}^{\chi_{c2}} - \Re\rho_{-2,-1}^{\chi_{c2}}) + \sqrt{6}(\Re\rho_{1,0}^{\chi_{c2}} - \Re\rho_{-1,0}^{\chi_{c2}})}{R_2}, \\ \lambda_{\theta'\phi'}^{\perp\chi_{c2}} &= \frac{2\sqrt{6}(\Im\rho_{0,2}^{\chi_{c2}} - \Im\rho_{0,-2}^{\chi_{c2}}) - 6\Im\rho_{1,-1}^{\chi_{c2}}}{R_2}, \\ \lambda_{\phi'}^{\perp\chi_{c2}} &= \frac{6(\Im\rho_{1,2}^{\chi_{c2}} + \Im\rho_{-1,-2}^{\chi_{c2}}) + \sqrt{6}(\Im\rho_{0,1}^{\chi_{c2}} + \Im\rho_{0,-1}^{\chi_{c2}})}{R_2}, \end{aligned} \quad (\text{C3})$$

with

$$\begin{aligned} R_1 &= [(15-2(a_2^{J=1})^2)N_{\chi_{c1}} \\ & - (5-6(a_2^{J=1})^2)\rho_{0,0}^{\chi_{c1}}]/(5-6(a_2^{J=1})^2), \\ R_2 &= [2(21+14(a_2^{J=2})^2+5(a_3^{J=2})^2)N_{\chi_{c2}} \\ & + 3(7-14(a_2^{J=2})^2-5(a_3^{J=2})^2)(\rho_{1,1}^{\chi_{c2}} + \rho_{-1,-1}^{\chi_{c2}}) \\ & + 4(7-14(a_2^{J=2})^2-5(a_3^{J=2})^2)\rho_{0,0}^{\chi_{c2}}] \\ & / (7-14(a_2^{J=2})^2-5(a_3^{J=2})^2). \end{aligned}$$

Appendix D: A possible way for determining $\rho_{J_z, J'_z}(|J_z - J'_z| > 2)$ of χ_{c2} with a reweighting method

From Eqs.(12), (14), (18), we see that the χ_{c2} SDMEs ρ_{J_z, J'_z} having $|J_z - J'_z| > 2$ cannot be measured from the integrated angular distributions. The fact that the coefficients of these SDMEs are suppressed by v^2 or $(m_{\chi_{c2}} - m_{J/\psi})$ makes the measurement of these polarization observables difficult. In this appendix, we propose a reweighting method to measure these SDMEs.

From Eq.(10), it can be recognized that this fact originates from the cancellation of the transverse and lon-

¹² If one does not integrate the angles θ and ϕ in the following equation and put the SDMEs $\rho_{s_z, s'_z}^{\chi_{cJ} \rightarrow J/\psi\gamma}(\theta, \phi)$ into Eq.(17), one obtains the full angular distribution of the decay chain $\chi_c \rightarrow J/\psi\gamma \rightarrow \mu^+\mu^-\gamma$, including the correlations between the χ_c decay angles θ, ϕ and the J/ψ decay angles θ', ϕ' , which might be useful in Monte Carlo simulations of experimental analyses.

itudinal components of the J/ψ coming from χ_{c2} .¹³ If the probabilities of the transverse and the longitudinal parts are made different by reweighting, the suppression of the $\rho_{J_z, J'_z}(|J_z - J'_z| > 2)$ terms can be avoided. The only tradeoff is that one should also measure the polar angle θ' of the μ^+ from the subsequent J/ψ decay.¹⁴ As is well known, the polar angle distribution of the μ^+ from the transverse polarized J/ψ decay is $\frac{(1+\cos^2\theta')}{2}$, while that from the longitudinal one is $(1 - \cos^2\theta')$. Therefore, after integrating over solid angles of the μ^+ , the transverse and longitudinal J/ψ components receive equal weight $D_{J_z, J'_z} = \sum_{\lambda_{J/\psi}=\pm, 0, \lambda_\gamma=\pm} \mathcal{M}_{J_z, \lambda_{J/\psi}, \lambda_\gamma} \mathcal{M}_{J'_z, \lambda_{J/\psi}, \lambda_\gamma}^*$ resulting in the cancellation of the terms containing $\rho_{J_z, J'_z}(|J_z - J'_z| > 2)$ of the χ_{c2} . It is possible to avoid these cancellations by measuring the angle θ' and assigning each reconstructed event the extra weight $w(\cos^2\theta')$. For example, if one chooses $w(\cos^2\theta') \propto \cos^2\theta'$, because of

$$\int d\cos\theta' (1 - \cos^2\theta') w(\cos^2\theta') : \int d\cos\theta' \frac{(1 + \cos^2\theta')}{2} w(\cos^2\theta') = 1 : 2,$$

the decay SDMEs become

$$D_{J_z, J'_z} = 2 \sum_{\lambda_{J/\psi}=\pm, \lambda_\gamma=\pm} \mathcal{M}_{J_z, \lambda_{J/\psi}, \lambda_\gamma} \mathcal{M}_{J'_z, \lambda_{J/\psi}, \lambda_\gamma}^* + \sum_{\lambda_\gamma=\pm} \mathcal{M}_{J_z, 0, \lambda_\gamma} \mathcal{M}_{J'_z, 0, \lambda_\gamma}^*, \quad (\text{D1})$$

and the cancellations do not occur. Without losing generality, we define r_L and r_T such that

$$\int d\cos\theta' (1 - \cos^2\theta') w(\cos^2\theta') : \int d\cos\theta' \frac{(1 + \cos^2\theta')}{2} w(\cos^2\theta') = r_L : r_T,$$

and

$$D_{J_z, J'_z} = r_T \sum_{\lambda_{J/\psi}=\pm, \lambda_\gamma=\pm} \mathcal{M}_{J_z, \lambda_{J/\psi}, \lambda_\gamma} \mathcal{M}_{J'_z, \lambda_{J/\psi}, \lambda_\gamma}^* + r_L \sum_{\lambda_\gamma=\pm} \mathcal{M}_{J_z, 0, \lambda_\gamma} \mathcal{M}_{J'_z, 0, \lambda_\gamma}^*. \quad (\text{D2})$$

The weighted angular distribution of $\chi_{c2} \rightarrow J/\psi\gamma$ is, thus,

$$\begin{aligned} \tilde{\mathcal{W}}^{\chi_{c2} \rightarrow J/\psi\gamma}(\theta, \phi) \propto & 1 + \lambda_\theta \cos^2\theta + \lambda_{2\theta} \cos^4\theta \\ & + \lambda_\phi \sin^2\theta \cos 2\phi + \lambda_\phi^\perp \sin^2\theta \sin 2\phi \\ & + \lambda_{\theta\phi} \sin 2\theta \cos \phi + \lambda_{\theta\phi}^\perp \sin 2\theta \sin \phi \\ & + \lambda_{2\phi} \sin^4\theta \cos 2\phi + \lambda_{2\phi}^\perp \sin^4\theta \sin 2\phi \\ & + \lambda_{2\theta\phi} \sin 2\theta \sin^2\theta \cos \phi \\ & + \lambda_{2\theta\phi}^\perp \sin 2\theta \sin^2\theta \sin \phi \\ & + \lambda_{3\theta\phi} \sin 2\theta \sin^2\theta \cos 3\phi \\ & + \lambda_{3\theta\phi}^\perp \sin 2\theta \sin^2\theta \sin 3\phi \\ & + \lambda_{4\phi} \sin^4\theta \cos 4\phi \\ & + \lambda_{4\phi}^\perp \sin^4\theta \sin 4\phi. \end{aligned} \quad (\text{D3})$$

The explicit expressions for the coefficients are

$$\begin{aligned} N_{\chi_{c2}} &= \rho_{2,2} + \rho_{1,1} + \rho_{0,0} + \rho_{-1,-1} + \rho_{-2,-2}, \\ R &= 3(r_T + r_L)N_{\chi_{c2}} + 3r_T(\rho_{1,1} + \rho_{-1,-1}) + (7r_T - 3r_L)\rho_{0,0}, \\ \lambda_\theta &= \frac{6r_T N_{\chi_{c2}} - 9r_L(\rho_{1,1} + \rho_{-1,-1}) - 6(5r_T - 3r_L)\rho_{0,0}}{R}, \\ \lambda_{2\theta} &= (r_T - r_L) \frac{3N_{\chi_{c2}} - 15(\rho_{1,1} + \rho_{-1,-1}) + 15\rho_{0,0}}{R}, \\ \lambda_\phi &= \left[2\sqrt{6}(4r_T - 3r_L)(\Re\rho_{2,0} + \Re\rho_{-2,0}) - 6(2r_T - 3r_L)\Re\rho_{1,-1} \right] / R, \\ \lambda_\phi^\perp &= - \left[2\sqrt{6}(4r_T - 3r_L)(\Im\rho_{2,0} - \Im\rho_{-2,0}) - 6(2r_T - 3r_L)\Im\rho_{1,-1} \right] / R, \\ \lambda_{\theta\phi} &= [6(2r_T - r_L)(\Re\rho_{2,1} - \Re\rho_{-2,-1}) - \sqrt{6}(2r_T - 3r_L)(\Re\rho_{1,0} - \Re\rho_{-1,0})] / R, \\ \lambda_{\theta\phi}^\perp &= - [6(2r_T - r_L)(\Im\rho_{2,1} + \Im\rho_{-2,-1}) - \sqrt{6}(2r_T - 3r_L)(\Im\rho_{1,0} + \Im\rho_{-1,0})] / R, \\ \lambda_{2\phi} &= (r_T - r_L) \frac{24\Re\rho_{1,-1} - 6\sqrt{6}(\Re\rho_{2,0} + \Re\rho_{-2,0})}{R}, \\ \lambda_{2\phi}^\perp &= -(r_T - r_L) \frac{24\Im\rho_{1,-1} - 6\sqrt{6}(\Im\rho_{2,0} - \Im\rho_{-2,0})}{R}, \\ \lambda_{2\theta\phi} &= 6(r_T - r_L) [-(\Re\rho_{2,1} - \Re\rho_{-2,-1}) + \sqrt{6}(\Re\rho_{1,0} - \Re\rho_{-1,0})] / R, \\ \lambda_{2\theta\phi}^\perp &= 6(r_T - r_L) [(\Im\rho_{2,1} + \Im\rho_{-2,-1}) - \sqrt{6}(\Im\rho_{1,0} + \Im\rho_{-1,0})] / R, \\ \lambda_{3\theta\phi} &= 6(r_T - r_L) \frac{\Re\rho_{2,-1} - \Re\rho_{-2,1}}{R}, \\ \lambda_{3\theta\phi}^\perp &= -6(r_T - r_L) \frac{\Im\rho_{2,-1} + \Im\rho_{-2,1}}{R}, \\ \lambda_{4\phi} &= (r_T - r_L) \frac{6\Re\rho_{2,-2}}{R}, \\ \lambda_{4\phi}^\perp &= -(r_T - r_L) \frac{6\Im\rho_{2,-2}}{R}. \end{aligned} \quad (\text{D4})$$

From the above equations, we find that one can measure $\lambda_{3\theta\phi}, \lambda_{3\theta\phi}^\perp, \lambda_{4\phi}, \lambda_{4\phi}^\perp$ to determine the values of $\rho_{J_z, J'_z}(|J_z - J'_z| > 2)$ if $r_T \neq r_L$.

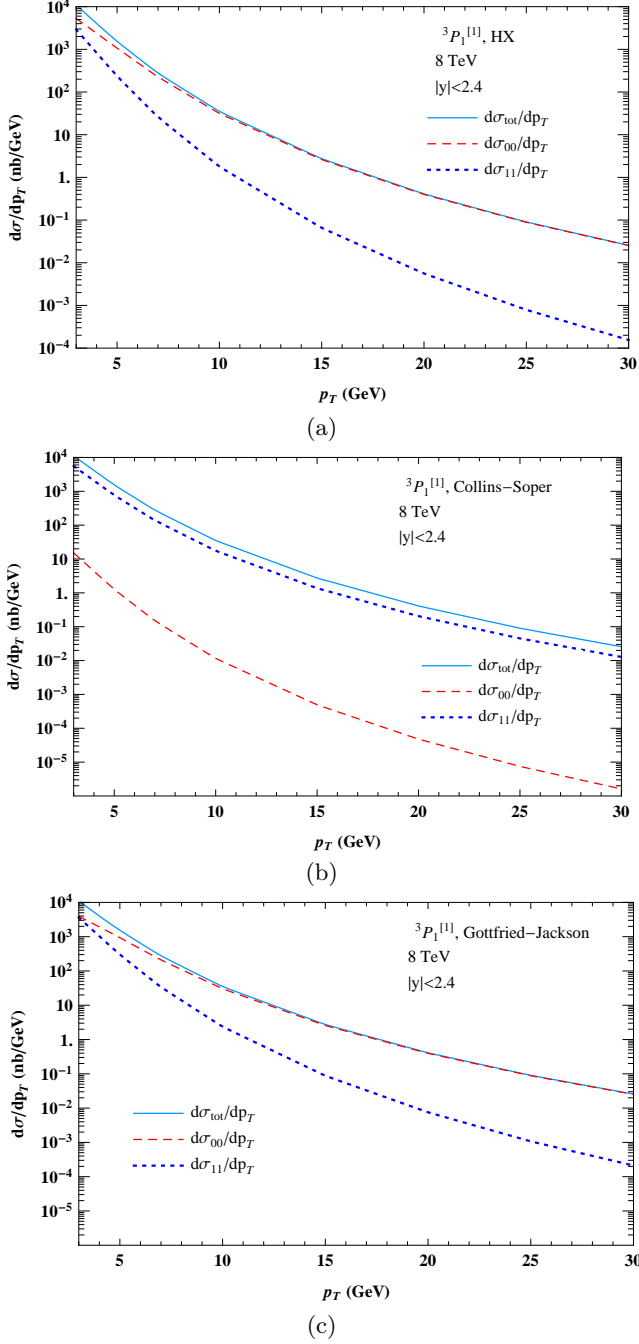
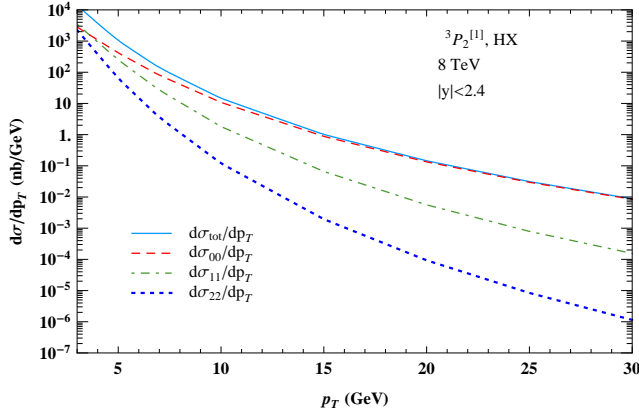


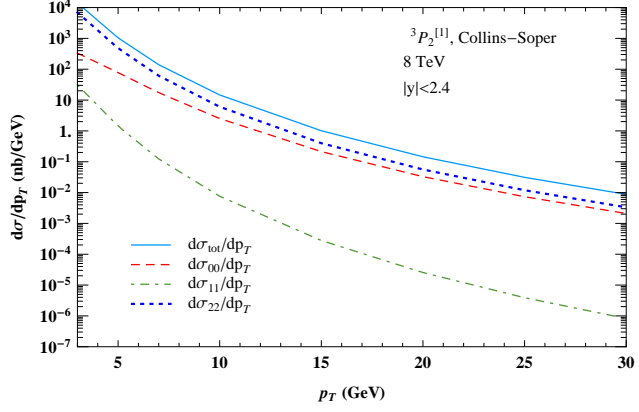
FIG. 3: (color online). Distributions of $\frac{d\sigma_{00}}{dp_T}$, $\frac{d\sigma_{11}}{dp_T}$, and $\frac{d\sigma_{\text{tot}}}{dp_T} = 2\frac{d\sigma_{11}}{dp_T} + \frac{d\sigma_{00}}{dp_T}$ for $^3P_1^{[1]}$ in the (a) HX, (b) Collins-Soper, and (c) Gottfried-Jackson frames.

-
- [1] N. Brambilla, S. Eidelman, B. Heltsley, R. Vogt, G. Bodwin, *et al.*, “Heavy quarkonium: progress, puzzles, and opportunities,” *Eur.Phys.J.* **C71** (2011) 1534, 1010.5827.
- [2] G. T. Bodwin, E. Braaten, and G. Lepage, “Rigorous QCD analysis of inclusive annihilation and production

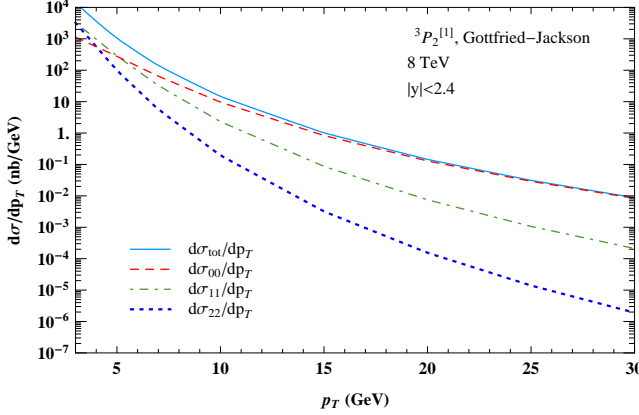
- of heavy quarkonium,” *Phys.Rev.* **D51** (1995) 1125–1171, hep-ph/9407339.
- [3] E. Braaten, B. A. Kniehl, and J. Lee, “Polarization of prompt J/ψ at the Tevatron,” *Phys.Rev.* **D62** (2000) 094005, hep-ph/9911436.
- [4] **CDF Collaboration** Collaboration, T. Affolder *et al.*,



(a)

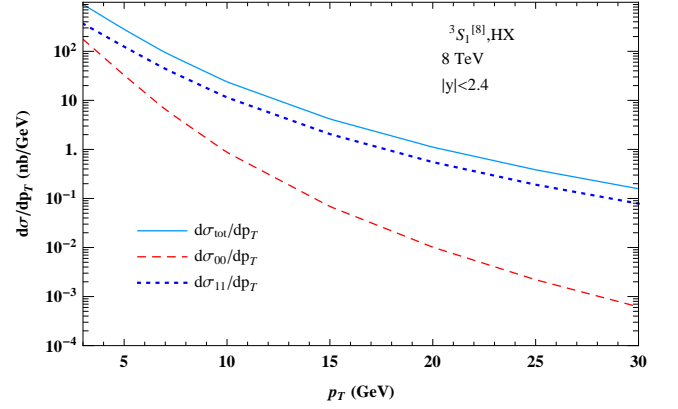


(b)

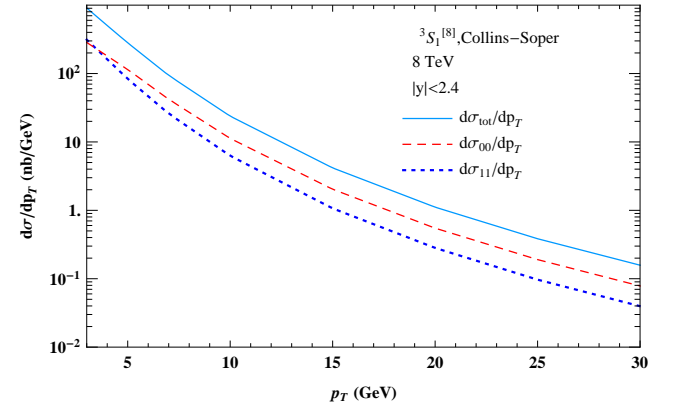


(c)

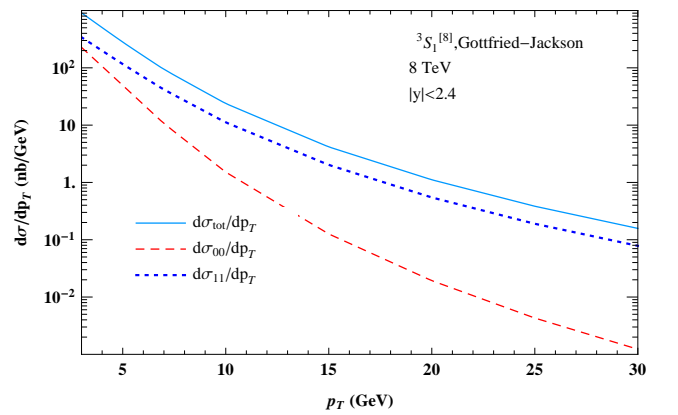
FIG. 4: (color online). Distributions of $\frac{d\sigma_{00}}{dp_T}$, $\frac{d\sigma_{11}}{dp_T}$, $\frac{d\sigma_{22}}{dp_T}$, and $\frac{d\sigma_{\text{tot}}}{dp_T} = 2\frac{d\sigma_{22}}{dp_T} + 2\frac{d\sigma_{11}}{dp_T} + \frac{d\sigma_{00}}{dp_T}$ for $^3P_2^{[1]}$ in the (a) HX, (b) Collins-Soper, and (c) Gottfried-Jackson frames.



(a)



(b)



(c)

FIG. 5: (color online). Distributions of $\frac{d\sigma_{00}}{dp_T}$, $\frac{d\sigma_{11}}{dp_T}$, and $\frac{d\sigma_{\text{tot}}}{dp_T} = 2\frac{d\sigma_{11}}{dp_T} + \frac{d\sigma_{00}}{dp_T}$ for $^3S_1^{[8]}$ [including only $\langle \mathcal{O}^{\chi_{c0}}(^3S_1^{[8]}) \rangle$] in the (a) HX, (b) Collins-Soper, and (c) Gottfried-Jackson frames.

“Measurement of J/ψ and $\psi(2S)$ polarization in $p\bar{p}$ collisions at $\sqrt{s} = 1.8$ TeV,” *Phys.Rev.Lett.* **85** (2000) 2886–2891, hep-ex/0004027.

- [5] **CDF Collaboration** Collaboration, A. Abulencia *et al.*, “Polarization of J/ψ and ψ_{2S} mesons produced in $p\bar{p}$ collisions at $\sqrt{s} = 1.96$ -TeV,” *Phys.Rev.Lett.* **99** (2007) 132001, 0704.0638.

- [6] P. Faccioli, C. Lourenco, J. Seixas, and H. K. Wohri, “Towards the experimental clarification of quarkonium

polarization,” *Eur.Phys.J.* **C69** (2010) 657–673, 1006.2738.

- [7] **CDF Collaboration** Collaboration, A. Abulencia *et al.*, “Measurement of $\sigma_{\chi_{c2}}\mathcal{B}(\chi_{c2} \rightarrow J/\psi\gamma)/\sigma_{\chi_{c1}}\mathcal{B}(\chi_{c1} \rightarrow J/\psi\gamma)$ in $p\bar{p}$ collisions at $\sqrt{s} = 1.96$ -TeV,” *Phys.Rev.Lett.* **98** (2007) 232001, hep-ex/0703028.
- [8] Y.-Q. Ma, K. Wang, and K.-T. Chao, “QCD radiative

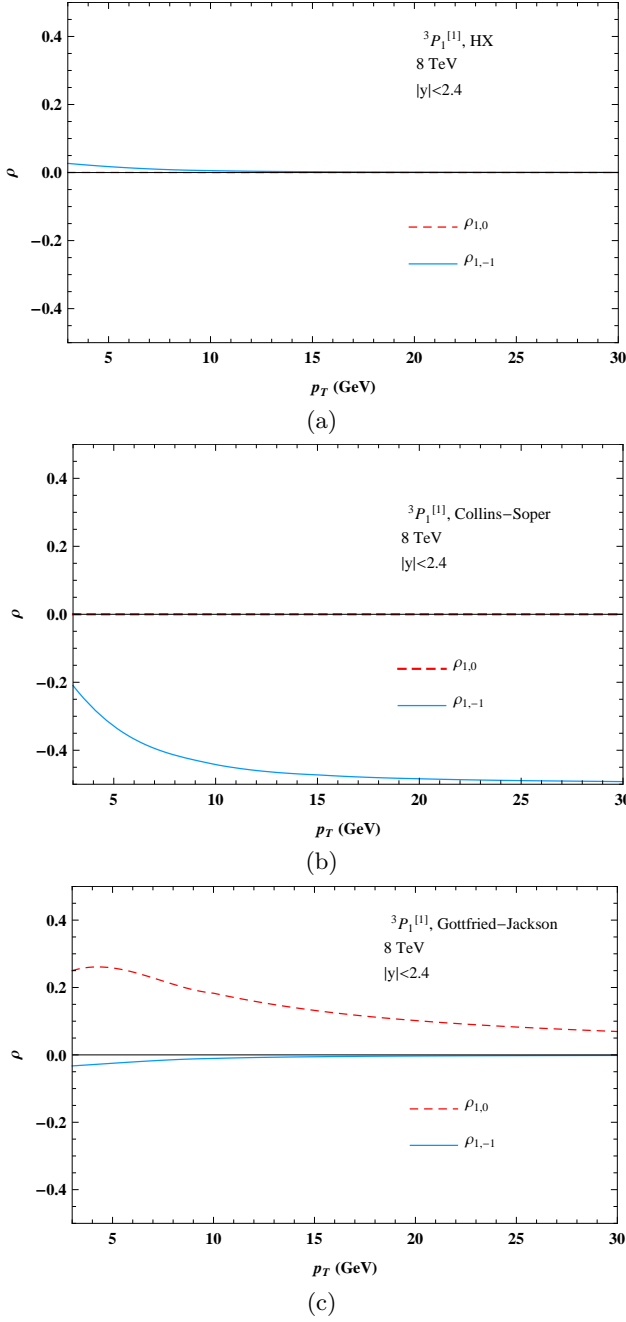


FIG. 6: (color online). Real parts of the nondiagonal SDMEs (normalized by $\frac{d\sigma_{\text{tot}}}{dp_T} = 2\frac{d\sigma_{11}}{dp_T} + \frac{d\sigma_{00}}{dp_T}$) for $^3P_1^{[1]}$ in the (a) HX, (b) Collins-Soper, and (c) Gottfried-Jackson frames.

corrections to χ_{cJ} production at hadron colliders,” *Phys.Rev.* **D83** (2011) 111503, 1002.3987.

- [9] **LHCb Collaboration** Collaboration, R. Aaij *et al.*, “Measurement of the cross-section ratio $\sigma(\chi_{c2})/\sigma(\chi_{c1})$ for prompt χ_c production at $\sqrt{s} = 7$ TeV,” *Phys.Lett.* **B714** (2012) 215–223, 1202.1080.
- [10] J. M. Campbell, F. Maltoni, and F. Tramontano, “QCD corrections to J/ψ and Upsilon production at hadron colliders,” *Phys.Rev.Lett.* **98** (2007) 252002,

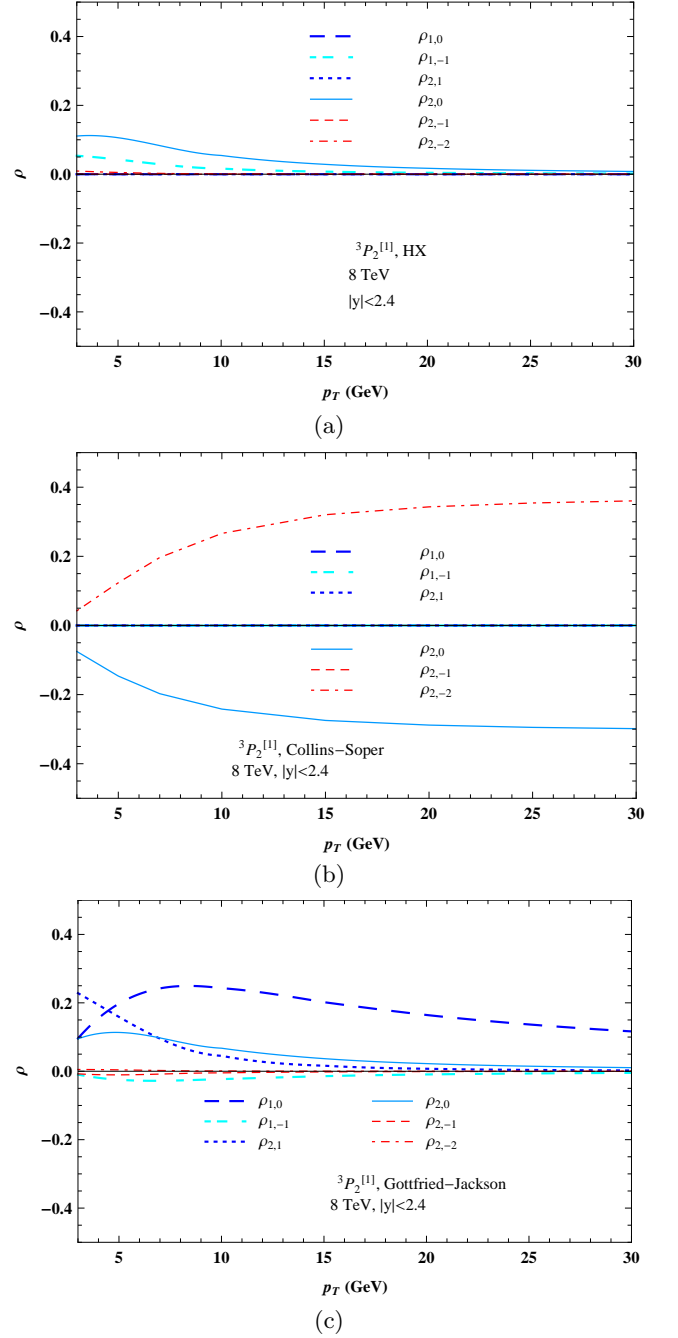


FIG. 7: (color online). Real parts of the nondiagonal SDMEs (normalized by $\frac{d\sigma_{\text{tot}}}{dp_T} = 2\frac{d\sigma_{22}}{dp_T} + 2\frac{d\sigma_{11}}{dp_T} + \frac{d\sigma_{00}}{dp_T}$) for $^3P_2^{[1]}$ in the (a) HX, (b) Collins-Soper, and (c) Gottfried-Jackson frames. In Fig.7(a), $\rho_{1,0}$, $\rho_{2,1}$, and $\rho_{2,-1}$ are almost zero. In Fig.7(b), $\rho_{1,0}$, $\rho_{1,-1}$, $\rho_{2,1}$, and $\rho_{2,-1}$ vanish.

hep-ph/0703113.

- [11] B. Gong, X. Q. Li, and J.-X. Wang, “QCD corrections to J/ψ production via color octet states at Tevatron and LHC,” *Phys.Lett.* **B673** (2009) 197–200, 0805.4751.
- [12] M. Butenschoen and B. A. Kniehl, “Reconciling J/ψ production at HERA, RHIC, Tevatron, and LHC with NRQCD factorization at next-to-leading order,”

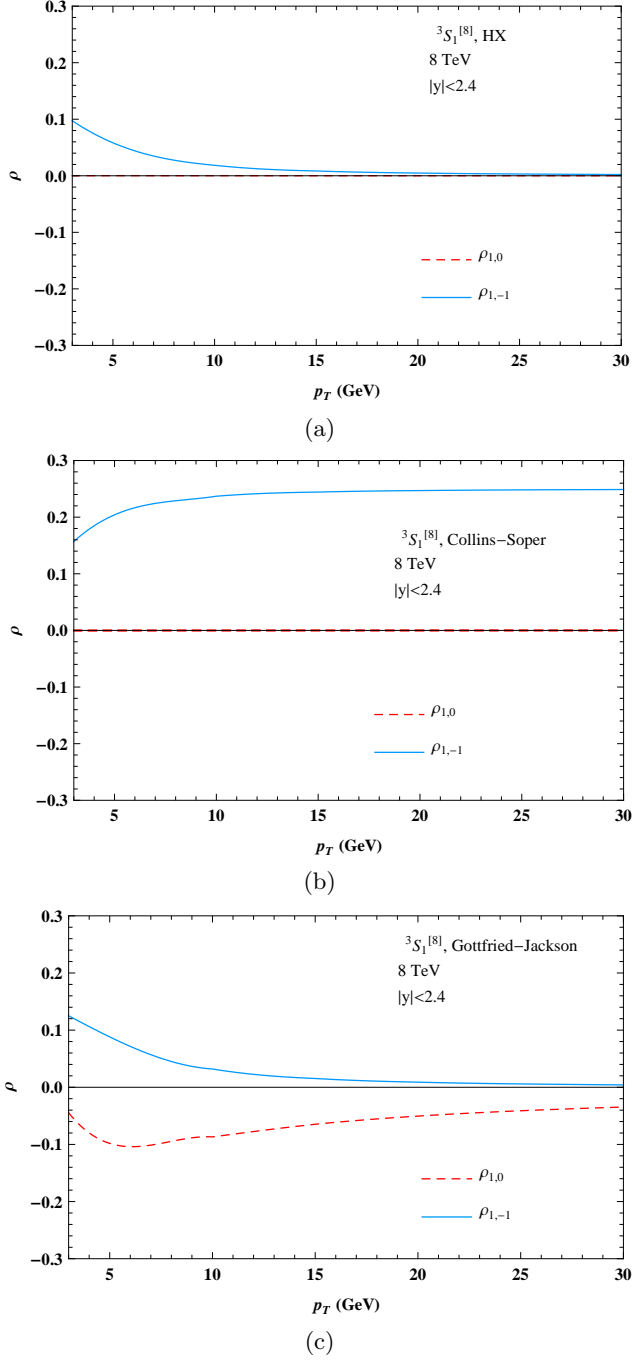


FIG. 8: (color online). Real parts of the nondiagonal SDMEs (normalized by $\frac{d\sigma_{\text{tot}}}{dp_T} = 2\frac{d\sigma_{11}}{dp_T} + \frac{d\sigma_{00}}{dp_T}$) for $^3S_1^{[8]}$ in the (a) HX, (b) Collins-Soper, and (c) Gottfried-Jackson frames.

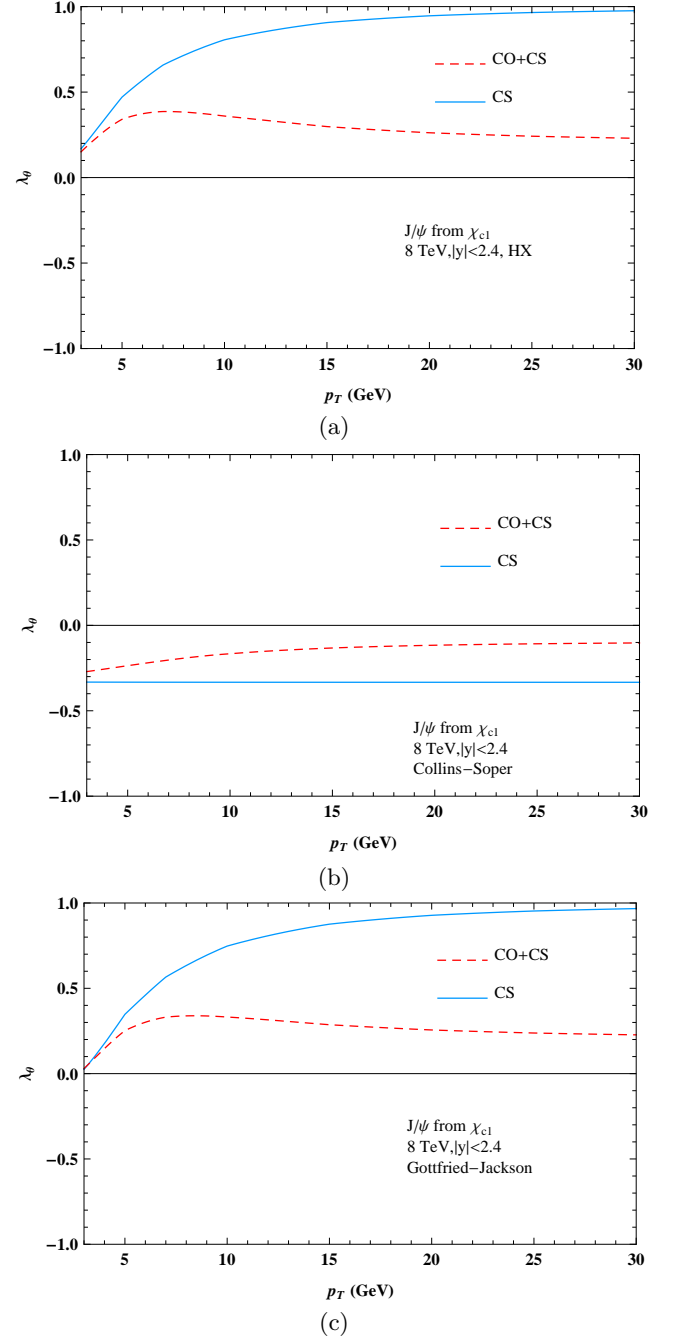
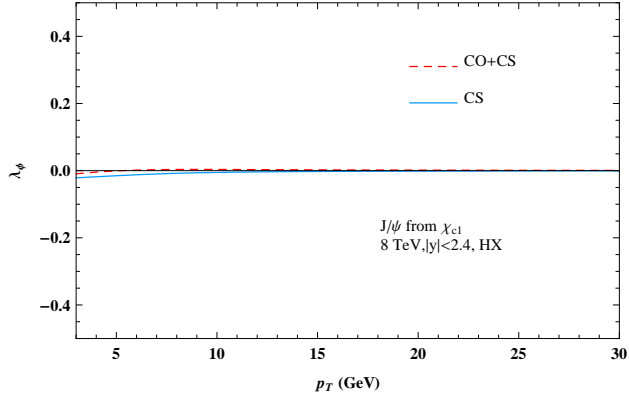


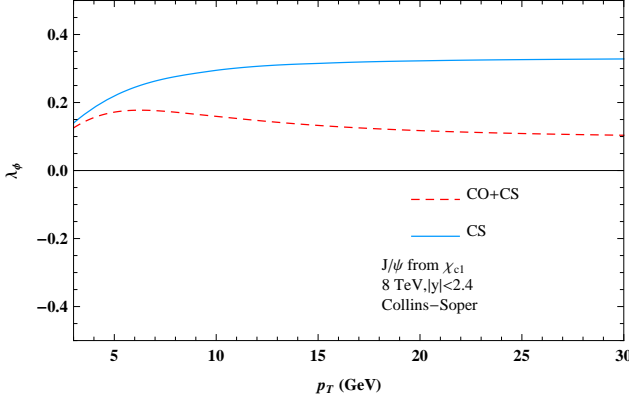
FIG. 9: (color online). Transverse momentum dependence of the parameter λ_θ of $\chi_{c1} \rightarrow J/\psi\gamma$ angular distribution, in the (a) HX, (b) Collins-Soper, and (c) Gottfried-Jackson frames.

- Phys.Rev.Lett.* **106** (2011) 022003, 1009.5662.
- [13] Y.-Q. Ma, K. Wang, and K.-T. Chao, “J/psi (psi’) production at the Tevatron and LHC at $O(\alpha_s^4 v^4)$ in nonrelativistic QCD,” *Phys.Rev.Lett.* **106** (2011) 042002, 1009.3655.
- [14] Y.-Q. Ma, K. Wang, and K.-T. Chao, “A complete NLO calculation of the J/ψ and ψ' production at hadron colliders,” *Phys.Rev.* **D84** (2011) 114001, 1012.1030.

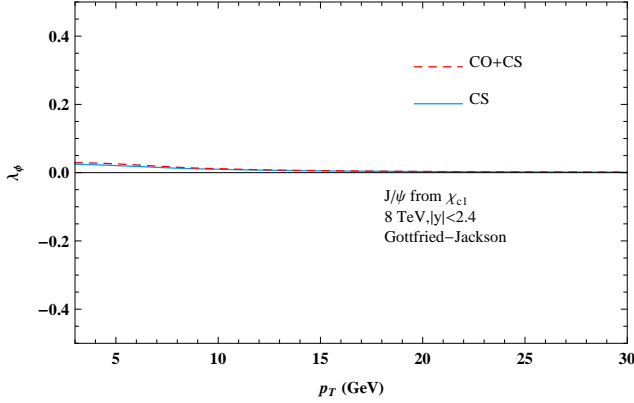
- [15] B. Gong and J.-X. Wang, “Next-to-leading-order QCD corrections to J/ψ polarization at Tevatron and Large-Hadron-Collider energies,” *Phys.Rev.Lett.* **100** (2008) 232001, 0802.3727.
- [16] Z.-B. Kang, J.-W. Qiu, and G. Sterman, “Heavy quarkonium production and polarization,” *Phys.Rev.Lett.* **108** (2012) 102002, 1109.1520. latex, 11 pages, 4 figures.
- [17] P. Artoisenet, J. M. Campbell, J. Lansberg, F. Maltoni,



(a)



(b)



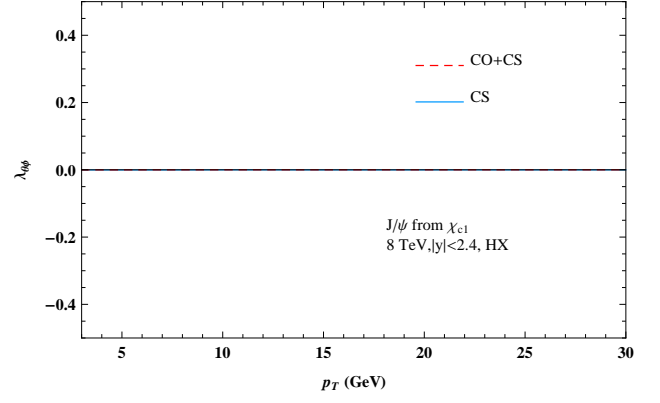
(c)

FIG. 10: (color online). Transverse momentum dependence of λ_ϕ of $\chi_{c1} \rightarrow J/\psi\gamma$ angular distribution, in the (a) HX, (b) Collins-Soper, and (c) Gottfried-Jackson frames.

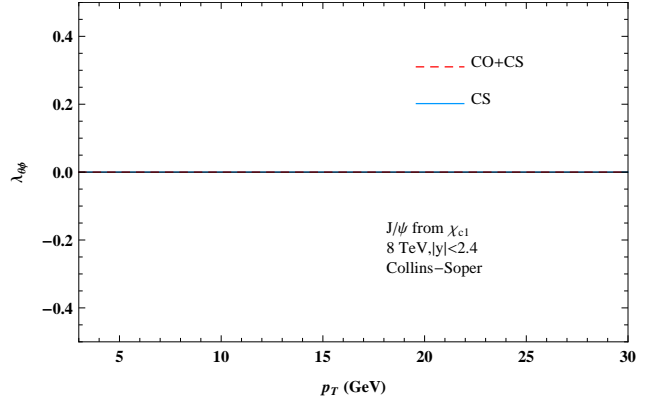
and F. Tramontano, “ Υ Production at Fermilab Tevatron and LHC Energies,” *Phys.Rev.Lett.* **101** (2008) 152001, 0806.3282.

- [18] M. Butenschoen and B. A. Kniehl, “J/psi polarization at Tevatron and LHC: Nonrelativistic-QCD factorization at the crossroads,” *Phys.Rev.Lett.* **108** (2012) 172002, 1201.1872.

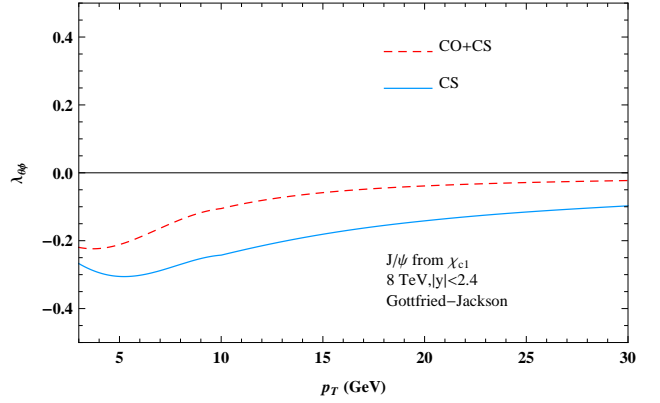
- [19] K.-T. Chao, Y.-Q. Ma, H.-S. Shao, K. Wang, and Y.-J. Zhang, “J/ψ polarization at hadron colliders in nonrelativistic QCD,” *Phys.Rev.Lett.* **108** (2012)



(a)



(b)



(c)

FIG. 11: (color online). Transverse momentum dependence of λ_{θ_ϕ} of $\chi_{c1} \rightarrow J/\psi\gamma$ angular distribution, in the (a) HX, (b) Collins-Soper, and (c) Gottfried-Jackson frames.

242004, 1201.2675.

- [20] **ATLAS Collaboration**, G. Aad *et al.*, “Measurement of the differential cross-sections of inclusive, prompt and non-prompt J/psi production in proton-proton collisions at $\sqrt{s} = 7$ TeV,” *Nucl. Phys.* **B850** (2011) 387–444, 1104.3038.
- [21] **CMS Collaboration**, S. Chatrchyan *et al.*, “J/psi and psi(2S) production in pp collisions at $\sqrt{s} = 7$ TeV,” *JHEP* **02** (2012) 011, 1111.1557.
- [22] B. A. Kniehl, G. Kramer, and C. P. Palisoc, “chi(c1)

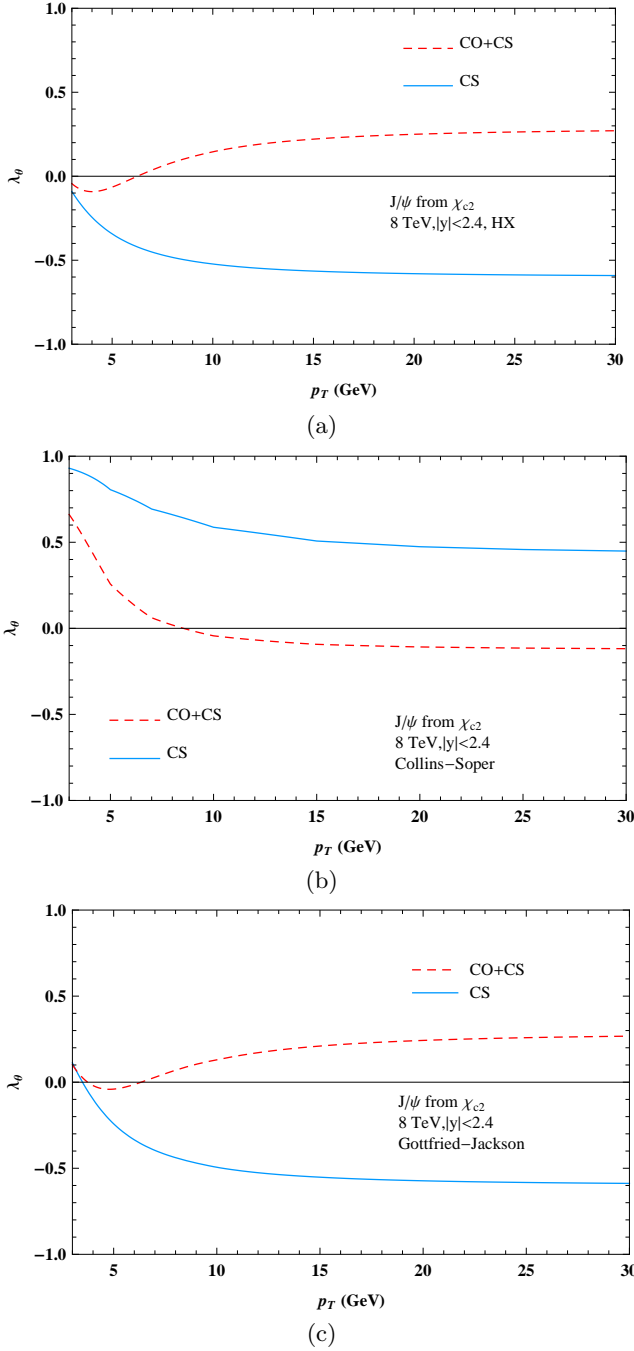


FIG. 12: (color online). Transverse momentum dependence of λ_θ of $\chi_{c2} \rightarrow J/\psi\gamma$ angular distribution, in the three polarization frames.

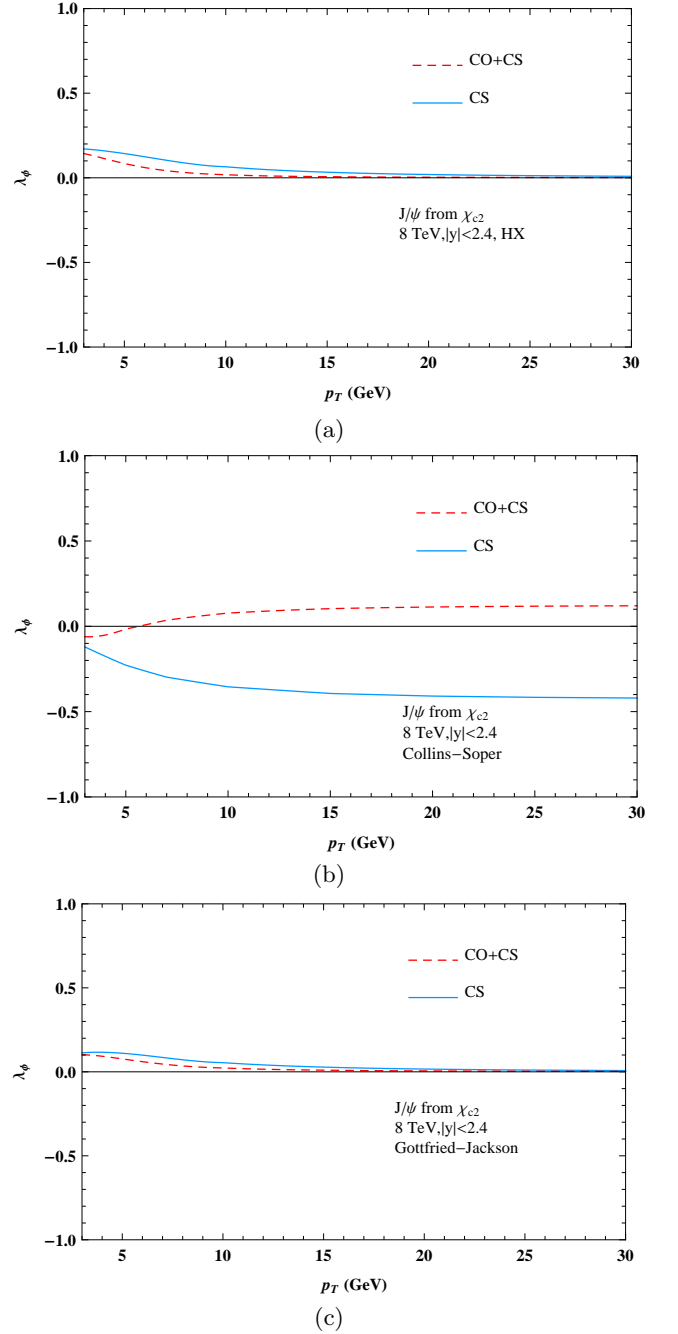


FIG. 13: (color online). Transverse momentum dependence of λ_ϕ of $\chi_{c2} \rightarrow J/\psi\gamma$ angular distribution, in the (a) HX, (b) Collins-Soper, and (c) Gottfried-Jackson frames.

and χ_{c2} decay angular distributions at the Fermilab Tevatron,” *Phys.Rev.* **D68** (2003) 114002, hep-ph/0307386.

- [23] P. Faccioli, C. Lourenco, J. Seixas, and H. K. Wohri, “Determination of χ_c and χ_b polarizations from dilepton angular distributions in radiative decays,” *Phys.Rev.* **D83** (2011) 096001, 1103.4882.
- [24] H. -S. Shao, Y. -Q. Ma, K. Wang and K. -T. Chao, “Polarizations of χ_{c1} and χ_{c2} in prompt production at

the LHC,” *Phys. Rev. Lett.* **112**, 182003 (2014) 1402.2913.

- [25] M. Beneke, M. Kramer, and M. Vanttinen, “Inelastic photoproduction of polarized J/ψ ,” *Phys.Rev.* **D57** (1998) 4258–4274, hep-ph/9709376.
- [26] E. Braaten, D. Kang, J. Lee, and C. Yu, “Optimal spin quantization axes for the polarization of dileptons with large transverse momentum,” *Phys.Rev.* **D79** (2009) 014025, 0810.4506.
- [27] E. Braaten, D. Kang, J. Lee, and C. Yu, “Optimal spin

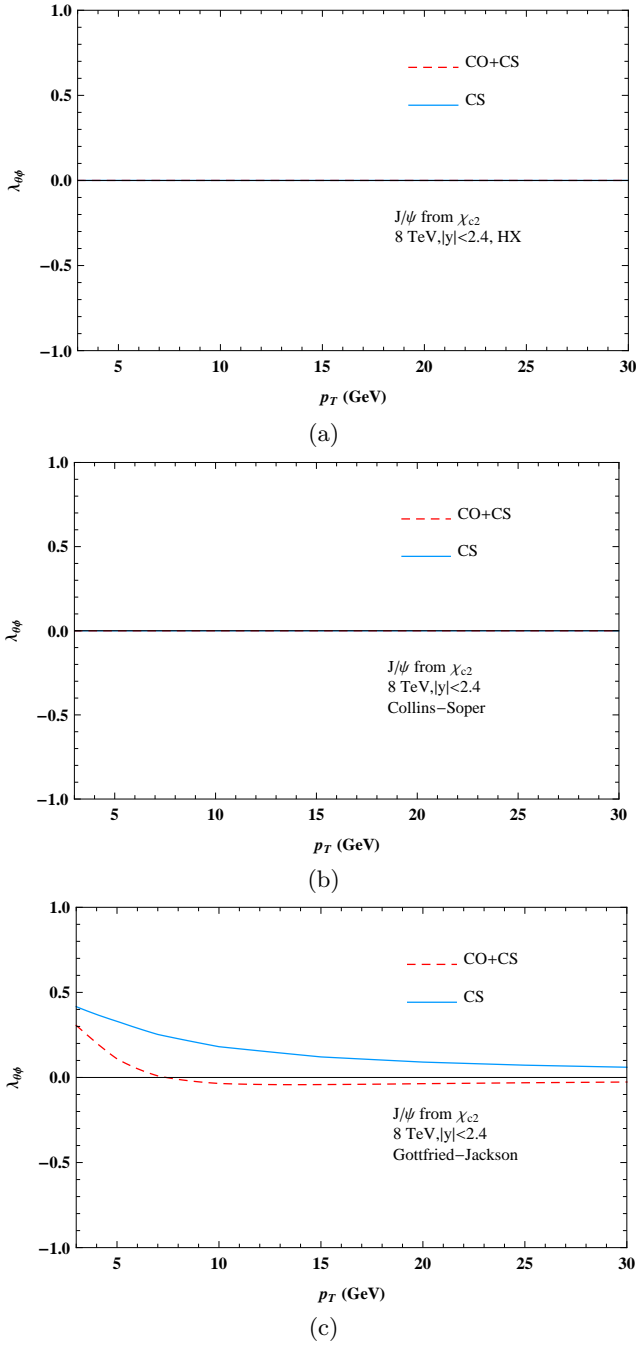


FIG. 14: (color online). Transverse momentum dependence of $\lambda_{\theta\phi}$ of $\chi_{c2} \rightarrow J/\psi\gamma$ angular distribution, in the (a) HX, (b) Collins-Soper, and (c) Gottfried-Jackson frames.

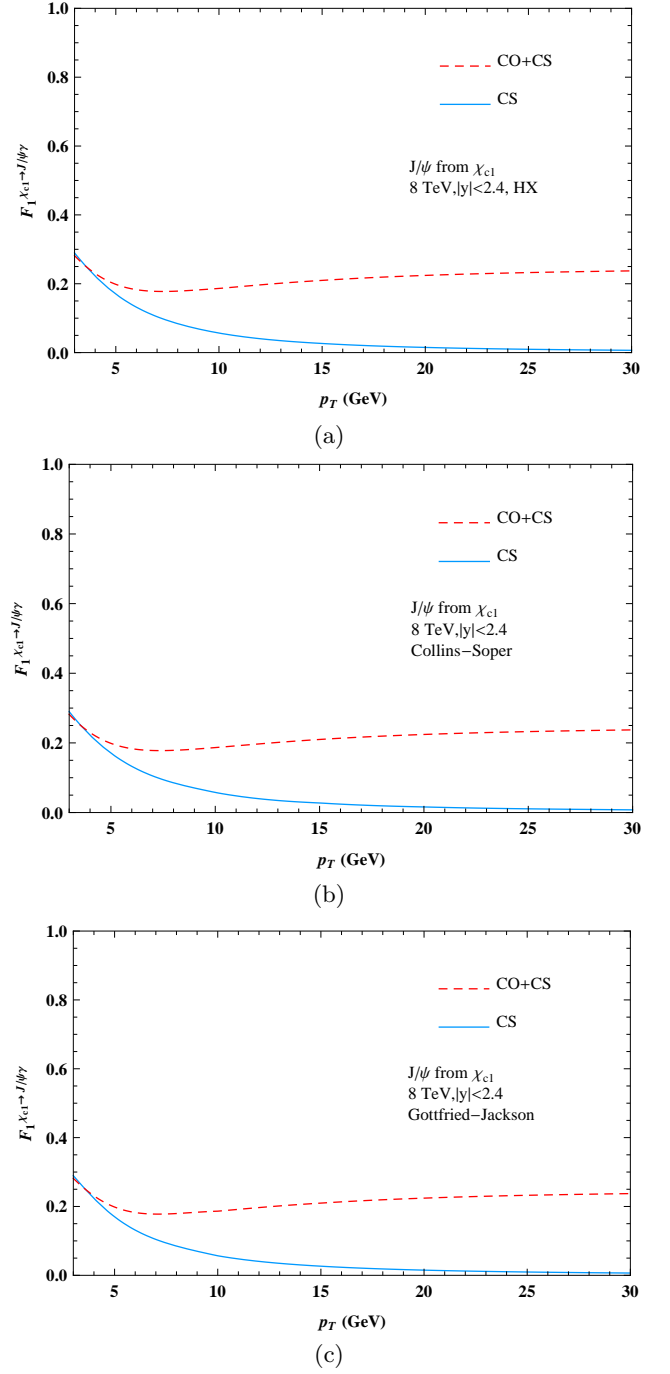


FIG. 15: (color online). Transverse momentum dependence of the frame-independent parameter $F_1^{\chi_{c1} \rightarrow J/\psi\gamma}$ [defined in Eq.(22)], in the (a) HX, (b) Collins-Soper, and (c) Gottfried-Jackson frames.

quantization axes for quarkonium with large transverse momentum,” *Phys.Rev.* **D79** (2009) 054013, 0812.3727.

- [28] **CMS Collaboration** Collaboration, S. Chatrchyan *et al.*, “Measurement of the Y1S, Y2S and Y3S polarizations in pp collisions at $\sqrt{s} = 7$ TeV,” *Phys.Rev.Lett.* **110** (2013) 081802, 1209.2922.
- [29] **CLEO Collaboration** Collaboration, M. Artuso *et al.*, “Higher-order multipole amplitudes in charmonium radiative transitions,” *Phys.Rev.* **D80** (2009) 112003,

0910.0046.

- [30] M. Oreglia, E. D. Bloom, F. Bulos, R. Chestnut, J. Gaiser, *et al.*, “A Study of the Reaction $\psi' \rightarrow \gamma\gamma J/\psi$,” *Phys.Rev.* **D25** (1982) 2259.
- [31] **E760 Collaboration** Collaboration, T. Armstrong *et al.*, “Study of the angular distribution of the reaction $\bar{p}p \rightarrow \chi_{c2} \rightarrow J/\psi\gamma \rightarrow e^+e^-\gamma$,” *Phys.Rev.* **D48** (1993)

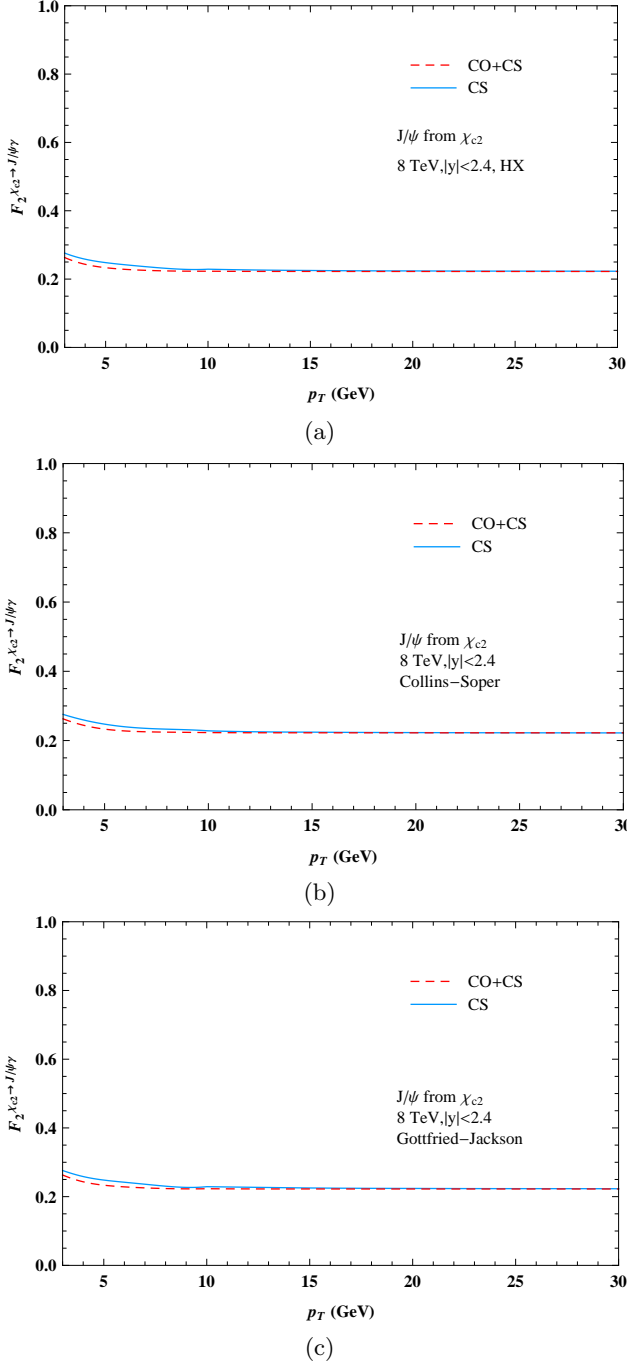


FIG. 16: (color online). Transverse momentum dependence of the frame-independent parameter $F_2^{\chi_{c2} \to J/\psi \gamma}$ [defined in Eq.(23)], in the (a) HX, (b) Collins-Soper, and (c) Gottfried-Jackson frames.

3037–3044.

- [32] **E835 Collaboration** Collaboration, M. Ambrogiani *et al.*, “Study of the angular distributions of the reactions $\bar{p}p \rightarrow \chi_{c1}, \chi_{c2} \rightarrow J/\psi \gamma \rightarrow e^+e^-\gamma$,” *Phys.Rev.* **D65** (2002) 052002.
- [33] C. Lam and W.-K. Tung, “A SYSTEMATIC APPROACH TO INCLUSIVE LEPTON PAIR

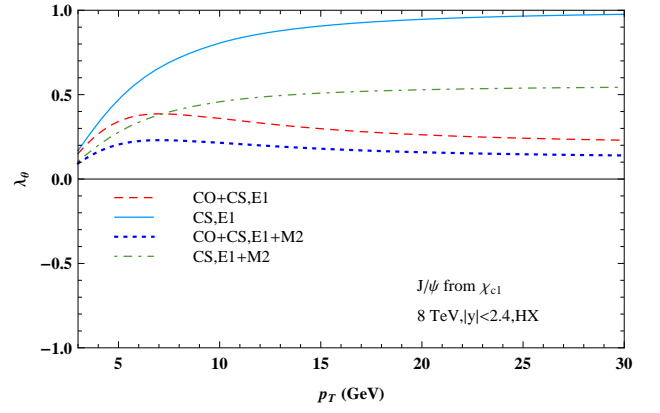


FIG. 17: (color online). M2 contribution to the χ_{c1} polarization λ_θ in $\chi_{c1} \rightarrow J/\psi \gamma$ in the HX frame. The CLEO measurement of $a^{J=1}$ listed in Table II has been used.

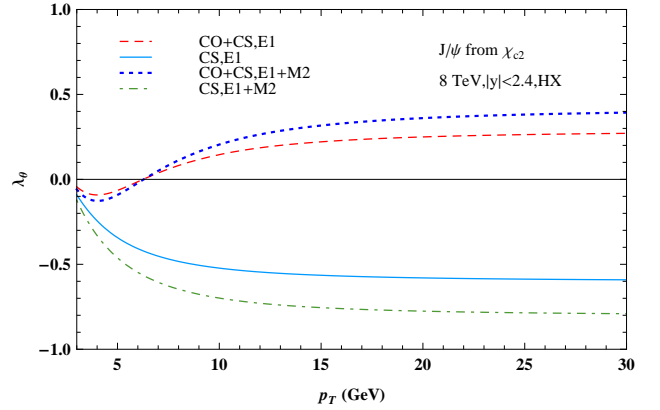


FIG. 18: (color online). M2 contribution to the χ_{c2} polarization λ_θ in $\chi_{c2} \rightarrow J/\psi \gamma$ in the HX frame. The CLEO measurement of $a_2^{J=2}$ listed in Table III has been used.

PRODUCTION IN HADRONIC COLLISIONS,” *Phys.Rev.* **D18** (1978) 2447.

- [34] C. Lam and W.-K. Tung, “A PARTON MODEL RELATION SANS QCD MODIFICATIONS IN LEPTON PAIR PRODUCTIONS,” *Phys.Rev.* **D21** (1980) 2712.
- [35] E. L. Berger, J.-W. Qiu, and R. A. Rodriguez-Pedraza, “Transverse momentum dependence of the angular distribution of the Drell-Yan process,” *Phys.Rev.* **D76** (2007) 074006, 0708.0578.
- [36] P. Faccioli, C. Lourenco, and J. Seixas, “Rotation-invariant relations in vector meson decays into fermion pairs,” *Phys.Rev.Lett.* **105** (2010) 061601, 1005.2601.
- [37] B. A. Kniehl and J. Lee, “Polarized J/ψ from $\chi(cJ)$ and ψ' decays at the Tevatron,” *Phys.Rev.* **D62** (2000) 114027, hep-ph/0007292.
- [38] P. Faccioli and J. Seixas, “Observation of χ_c and χ_b nuclear suppression via dilepton polarization measurements,” *Phys.Rev.* **D85** (2012) 074005, 1203.2033.
- [39] S. Chung and T. Trueman, “Positivity Conditions on

- the Spin Density Matrix: A Simple Parametrization,” *Phys.Rev.* **D11** (1975) 633.
- [40] **CDF Collaboration** Collaboration, F. Abe *et al.*, “Production of J/ψ mesons from χ_c meson decays in $p\bar{p}$ collisions at $\sqrt{s} = 1.8$ TeV,” *Phys.Rev.Lett.* **79** (1997) 578–583.
- [41] E. J. Eichten and C. Quigg, “Quarkonium wave functions at the origin,” *Phys.Rev.* **D52** (1995) 1726–1728, hep-ph/9503356.
- [42] H.-S. Shao, “HELAC-Onia: An automatic matrix element generator for heavy quarkonium physics,” *Comput.Phys.Commun.* **184** (2013) 2562–2570, 1212.5293.
- [43] A. Kanaki and C. G. Papadopoulos, “HELAC: A package to compute electroweak helicity amplitudes,” *Comput. Phys. Commun.* **132** (2000) 306–315, hep-ph/0002082.
- [44] C. Papadopoulos and M. Worek, “HELAC - A Monte Carlo generator for multi-jet processes,” hep-ph/0606320.
- [45] C. G. Papadopoulos, “PHEGAS: A phase space generator for automatic cross- section computation,” *Comput. Phys. Commun.* **137** (2001) 247–254, hep-ph/0007335.
- [46] A. Cafarella, C. G. Papadopoulos, and M. Worek, “Helac-Phegas: a generator for all parton level processes,” *Comput. Phys. Commun.* **180** (2009) 1941–1955, 0710.2427.
- [47] R. Kleiss, W. Stirling, and S. Ellis, “A NEW MONTE CARLO TREATMENT OF MULTIPARTICLE PHASE SPACE AT HIGH-ENERGIES,” *Comput.Phys.Commun.* **40** (1986) 359.
- [48] G. Lepage, “A New Algorithm for Adaptive Multidimensional Integration,” *J.Comput.Phys.* **27** (1978) 192. Revised version.
- [49] J. Pumplin, D. Stump, J. Huston, H. Lai, P. M. Nadolsky, *et al.*, “New generation of parton distributions with uncertainties from global QCD analysis,” *JHEP* **0207** (2002) 012, hep-ph/0201195.
- [50] E. Braaten and T. C. Yuan, “Gluon fragmentation into P wave heavy quarkonium,” *Phys.Rev.* **D50** (1994) 3176–3180, hep-ph/9403401.
- [51] B. Gong, L.-P. Wan, J.-X. Wang, and H.-F. Zhang, “Polarization for Prompt J/ψ , $\psi(2s)$ production at the Tevatron and LHC,” *Phys.Rev.Lett.* **110** (2013) 042002, 1205.6682.